MOLECULAR AND CELLULAR BIOLOGY, Mar. 2008, p. 1947–1963 Vol. 28, No. 6
0270-7306/08/$08.00+0 doi:10.1128/MCB.01672-07

Epidermal Growth Factor-Dependent Phosphorylation and Ubiquitinylation of MAGE-11 Regulates Its Interaction with the Androgen Receptor[▽]

Suxia Bai and Elizabeth M. Wilson*

Laboratories for Reproductive Biology, Lineberger Comprehensive Cancer Center, and Departments of Pediatrics and Biochemistry and Biophysics, University of North Carolina, Chapel Hill, North Carolina 27599

Received 10 September 2007/Returned for modification 9 October 2007/Accepted 7 January 2008

The androgen receptor (AR) is a ligand-activated transcription factor that interacts with coregulatory proteins during androgen-dependent gene regulation. Melanoma antigen gene protein 11 (MAGE-11) is an AR coregulator that specifically binds the AR NH_2-terminal FXXLF motif and modulates the AR NH_2- and carboxyl-terminal N/C interaction to increase AR transcriptional activity. Here we demonstrate that epidermal growth factor (EGF) signaling increases androgen-dependent AR transcriptional activity through the post-translational modification of MAGE-11. EGF in the presence of dihydrotestosterone stabilizes the AR-MAGE complex through the site-specific phosphorylation of MAGE-11 at Thr-360 and ubiquitinylation at Lys-240 and Lys-245. The time-dependent EGF-induced increase in AR transcriptional activity by MAGE-11 is mediated through AR activation functions 1 and 2 in association with the increased turnover of AR and MAGE-11. The results reveal a dynamic mechanism whereby growth factor signaling increases AR transcriptional activity through the covalent modification of an AR-specific coregulatory protein. Sequence conservation of the MAGE-11 phosphorylation and ubiquitinylation sites throughout the MAGE gene family suggests common regulatory mechanisms for this group of cancer-testis antigens.

The androgen receptor (AR) is a ligand-dependent transcription factor that mediates the effects of the biologically active androgens testosterone and dihydrotestosterone (DHT) on gene regulation required for male sex development and function. Androgen-dependent gene regulation involves interactions between AR and androgen response element DNA and coregulatory proteins that link to the transcriptional machinery of chromatin. Like other steroid receptors, AR has a multidomain structure that includes the NH_2-terminal activation domain 1 (AF1), which has evolved during mammalian evolution (9, 11) and is considered predominant in AR function. Activation function 2 (AF2) in the ligand binding domain functions as a binding site for SRC/p160 coactivator LXXLL motifs and for the FXXLF motif in the AR NH_2 terminus and in several putative AR coregulatory proteins (23, 25, 27). Cell-free fluorescence binding studies have shown that the AR20-30 FXXLF motif peptide binds to AF2 with 5- to 10-fold-higher affinity than an LXXLL motif containing a peptide from the most active ARSRC/p160 coactivator (23) and is the basis of the androgen-dependent AR NH_2-terminal and carboxyl-terminal (N/C) interaction important for androgen-induced gene activation (7, 25, 26, 30, 40). The AR N/C interaction slows the dissociation rate of bound androgen (62), stabilizes AR binding to androgen response element DNA (60), and appears to be involved in domain swapping between an intramolecular AR monomer in the cytoplasm and an intermolecular antiparallel AR dimer in the nucleus (39, 51). The importance of the N/C interaction for AR function is supported by studies on the human androgen insensitivity syndrome, in which naturally occurring single amino acid mutations in AF2 reduce binding of the AR FXXLF and SRC/p160 LXXLL motifs without altering the apparent equilibrium androgen binding affinity (15, 22, 34, 49). The different physiological potencies of testosterone and DHT have been linked to ligand-specific effects transmitted to the AF2 surface, where the weaker potency of testosterone, a more polarized steroid than DHT, derives from its inability to fully stabilize the AF2 binding surface for AR FXXLF and SRC/p160 coactivator LXXLL motif binding (1).

Recently, we demonstrated that the androgen-dependent AR N/C interaction is modulated by the AR coregulatory protein, melanoma antigen gene protein 11 (MAGE-11) of the MAGE-A gene family (3). MAGE-11 was identified in a two-hybrid screen of a human testis library using the AR FXXLF motif and flanking sequence as bait. MAGE-11 binds the AR NH_2-terminal FXXLF motif region, competes for the AR N/C interaction, and increases AR transcriptional activity in part by exposing AF2 for SRC/p160 coactivator recruitment. MAGE-11 binding to the AR FXXLF motif is selective. MAGE-11 does not interact with the FXXLF motif regions present in the putative AR coregulators ARA-70, ARA-54, and ARA-55, even though these same FXXLF motifs mediate coactivator interaction with the AR AF2 site (3, 27). Based on coimmunoprecipitation experiments, AR and MAGE-11 form a stable complex in the absence of androgen, but their association is transient in the presence of androgen (3). These results brought into question the mechanisms whereby MAGE-11 modulates androgen-induced gene regulation by AR. We have also shown that epidermal growth factor (EGF) can increase AR transcriptional activity through mechanisms that involve coactivators (16), and EGF receptor signaling has been linked to increased AR tran-

* Corresponding author. Mailing address: Laboratories for Reproductive Biology, CB 7500, University of North Carolina, Chapel Hill, NC 27599-7500. Phone: (919) 966-5168. Fax: (919) 966-2203. E-mail: emw@med.unc.edu.

▽ Published ahead of print on 22 January 2008.

scriptional activity in prostate cancer (12, 43). There is also evidence in prostate cancer cells for ligand-independent activation of AR through second messengers (13).

In this report we sought to identify the underlying mechanisms that account for the transient nature of the MAGE-AR-DHT complex. Our studies demonstrate that EGF promotes the formation of a more stable MAGE-AR-DHT complex through site-specific ubiquitinylation at two lysine residues required for MAGE-11 to interact with the AR FXXLF motif. EGF-induced ubiquitinylation of MAGE-11 is linked to phosphorylation of MAGE-11, more rapid turnover of AR and MAGE-11, and increased AR transcriptional activity.

MATERIALS AND METHODS

Plasmids. pCMVhAR (pCMV-AR), coding for full-length human AR amino acid residues 1 to 919 (45), pCMV-AR1-660 (53), VP-AR1-660 (25), GAL-AR16-36 (28), pSG5-MAGE-1-429, coding for full-length MAGE-11 (pSG5-MAGE), Flag-MAGE-2-429 (Flag-MAGE), GAL-MAGE-2-429 (GAL-MAGE), VP-MAGE-2-429 (VP-MAGE) (3), and pSG5-TIF2 (59) were previously described. Flag-ubiquitin (Flag-Ub), coding for a single ubiquitin protein, was kindly provided by Stephanie L. H. Miller and John P. O'Bryan. pSG5-6His-HA-Ub-KO, coding for lysine-free ubiquitin and in which all lysine residues are converted to arginine, was kindly provided by David Lonard and Bert O'Malley. Flag-Ub-KO, coding for lysine-free ubiquitin with all lysines mutated to arginine, was created by subcloning Ub-2-76-KO into the HindIII/BamHI sites of pCMV-Flagb. Mutagenic primers were used in single and double PCRs to prepare the AR and MAGE-11 mutants. pCMV-ARΔ120–472 was created by double PCR mutagenesis of pCMV-AR with the BglII/KpnI fragment inserted at the same sites of pCMV-AR.

pSG5-MAGEΔ221–249 and pSG5-MAGE with single mutations K225A, K236A, and K245A, double mutation K240A,K245A, and triple mutation K236A,K240A,K245A were created by double PCR mutagenesis using pSG5-MAGE as template and inserting the EcoRI/BglII-digested fragments into the same sites in pSG5-MAGE. pSG5-MAGE-K225A,K236A,K240A,K245A was created by double PCR mutagenesis of pSG5-MAGE-K236A,K240A,K245A and the EcoRI/BglII-digested fragment inserted into the same sites in pSG5-MAGE-K236A,K240A,K245A. pSG5-MAGE serine- and threonine-to-alanine mutants were created using pSG5-MAGE as template by double PCR site-specific mutagenesis or by QuikChange site-directed mutagenesis (Stratagene). PCR-amplified fragments were digested with EcoRI/XhoI (S174A and S168A,S170A, S174A) or EcoRI/BglII and inserted into the same sites of pSG5-MAGE.

pSG5-HA-MAGE-112-429, pSG5-HA-MAGE-2-429Δ221–249 (HA-MAGEΔ221–249), and pSG5-HA-MAGE-112-429 with mutations K236A, K240A, T360A, and K236A,K240A,K245A were created by PCR amplifying the corresponding wild-type or mutant pSG5-MAGE and inserting the EcoRI/XhoI-digested fragments into the same sites of pSG5-HA that code for a fusion protein linked to the NH_2-terminal human influenza virus hemagglutinin (HA) tag. pSG5-HA-MAGE-2-252, wild-type and mutant pSG5-HA-MAGE-112-362, and pSG5-HA-MAGE-2-362 were created by PCR mutagenesis of the corresponding pSG5-MAGE mutants and inserting the EcoRI/SalI-digested fragment into the EcoRI/XhoI sites of pSG5-HA. pSG5-HA-MAGE-112-362-T360A was created by QuikChange site-directed mutagenesis. pSG5-HA-MAGE-112-429-S168A, S170A,S174A,S181A,S199A,S208A (6-SA) was created by sequentially introducing the S208A, S181A, and S199A mutations into pSG5-HA-MAGE-112-429-S168A,S170A,S174A by cloning the PCR-amplified fragments into the EcoRI/XhoI sites.

Flag-MAGEΔ221–249 and Flag-MAGE with K240A, K225A,K236A,K240A, K245A, and T360A mutations were created by PCR amplifying the corresponding mutants in pSG5-MAGE and inserting the EcoRI/XhoI-digested fragments into the EcoRI/SalI sites of pCMV5-Flagb. VP-MAGEΔ221–249 and GAL-MAGEΔ221–249 were created by PCR amplifying pSG5-MAGEΔ221–249 and inserting the EcoRI/XhoI-digested fragments into the EcoRI/SalI sites of pVP16 and GAL-0. All PCR-amplified regions were verified by DNA sequencing.

DNA transfection in cultured cells. Monkey kidney CV1 cells were maintained and transfected using calcium phosphate DNA precipitation as described elsewhere (21, 22). CV1 cells (4.2×10^5 cells/6-cm dish) were transfected with 0.1 μg pCMV-AR or 0.1 μg pCMV-ARΔ120–472 in the absence and presence of 2 μg pSG5-TIF2, 1 or 2 μg wild-type or mutant pSG5-MAGE, and 5 μg prostate-specific antigen enhancer luciferase (PSA-Enh-Luc) or 5 μg mouse mammary tumor virus luciferase (MMTV-Luc) reporter vectors. After transfection, CV1 cells were placed in serum-free, phenol red-free medium in the absence and presence of 1 nM DHT. Twenty-four h later, the media with and without DHT were exchanged, and the next day luciferase activity was measured.

The effects of wild-type and mutant MAGE-11 on AR AF1 constitutive activity were determined in HeLa cells maintained and transfected using FuGENE-6 transfection reagent (Roche Applied Science) as described previously (1). HeLa cells (5×10^4 cells/well in 12-well plates) were transfected with 0.1 μg PSA-Enh-Luc and 0.01 μg pCMV-AR1-660 in the absence and presence of 0.1 μg wild-type or mutant pSG5-MAGE. The following day the medium was changed to serum-free, phenol red-free medium, and cells were incubated for another 24 h before measuring luciferase activity.

Two hybrid interaction assays were performed in HeLa cells using FuGENE-6 as described elsewhere (1). HeLa cells (5×10^4 cells/well in 12-well plates) were transfected with 0.1 μg 5XGAL4Luc3 luciferase reporter vector, 0.05 μg wild-type or mutant GAL-MAGE or VP-MAGE, and 0.05 μg pVP16, VP-AR1-660, or GAL-AR16-36. The next day the medium was changed to serum-free, phenol red-free medium, and luciferase activity was measured after 24 h.

Human endometrial Ishikawa cells were maintained in Eagle's minimum essential medium supplemented with 10% fetal bovine serum, penicillin, streptomycin, and 2 mM L-glutamine. Ishikawa cells (10^5 cells/well in 12-well plates) were transfected using FuGENE-6 with 0.1 μg PSA-Enh-Luc or 0.1 μg MMTV-Luc with 0.01 μg pCMV-AR or pCMV-AR1-660 in the absence and presence of 0.1 μg wild-type and mutant pSG5-MAGE (2). After 24 h, cells were treated in serum-free, phenol red-free medium for 24 h in the absence and presence of EGF. For small interfering RNA (siRNA) experiments, Ishikawa cells (7.5×10^4 cells/well in 12-well plates) were transfected in antibiotic-free medium using Lipofectamine 2000 reagent (Invitrogen) with 0.1 μg MMTV-Luc and 0.025 μg pCMV-AR in the absence and presence of 2 nM MAGE-11 siRNA with the following sense sequences: siRNA-1, GGAGGGAUCCCACUUCUUAUU; siRNA-2, GCACUGAUCCUGCAUGCUAUU; siRNA-3, CAACUGCUCUU UGGCAUUGUU (Dharmacon RNA Technologies). The next day cells were placed in serum-free, phenol red-free medium without hormone treatment. After 24 h the medium was replaced with and without 0.1 nM DHT and 10 ng/ml EGF, cells were cultured for another 24 h, and luciferase activity was measured.

For transfections in CV1, HeLa, and Ishikawa cells, luciferase activity was determined using a Lumistar Galaxy automated multiwell plate reader luminometer (BMG Labtech). All of the luciferase data are representative of at least three independent experiments.

Immunochemical procedures. Immunoprecipitation and immunoblotting experiments were performed using monkey kidney COS-1 cells maintained in Dulbecco's modified Eagle's medium and transfected in 10-cm dishes using DEAE dextran as described previously (21). For each coimmunoprecipitation, two 10-cm dishes containing 1.8×10^6 to 2.5×10^6 COS cells were transfected with the indicated amounts of Flagb empty vector, wild-type and mutant Flag-MAGE, Flag-Ub and Flag-Ub-KO with and without pCMV-AR, and wild-type and mutant pSG5-HA-MAGE and pooled. For phosphothreonine analysis, COS cells were transfected with wild-type pSG5-HA-MAGE-112-429 and the T360A mutant. Twenty-four h after transfection, cells were placed in serum-free, phenol red-free medium for the indicated times in the absence and presence of DHT and EGF and harvested in 1 ml phosphate-buffered saline (PBS)/10-cm dish. Cells were pelleted by centrifugation and solubilized in 1 ml immunoprecipitation (IP) lysis buffer containing 0.15 M NaCl, 0.5% NP-40, 50 mM NaF, 50 mM Tris-HCl, pH 7.5, 1 mM dithiothreitol, 1 mM phenylmethylsulfonyl fluoride, and protease inhibitor cocktail (Roche). Protein extracts were precleared with 100 μl agarose (Sigma), and extracts were incubated with 15 μl anti-Flag M2 affinity gel (Sigma) for 1 to 2 h or overnight at 4°C and washed four times with IP lysis buffer. For phosphothreonine analysis, extraction buffer contained, in addition, phosphatase inhibitor cocktail 1 and 2 (Sigma), and equivalent amounts of protein extract were immunoprecipitated using anti-HA affinity matrix (rat polyclonal; 15 μl resin/470 μg protein; Roche). Adsorbed proteins were released in 50 μl 2$\times$ sample buffer (3.3% sodium dodecyl sulfate [SDS], 10% glycerol, 10% 2-mercaptoethanol, and 0.12 M Tris-HCl, pH 6.8) and analyzed by immunoblotting as described elsewhere (3) in 10% acrylamide gels containing SDS. Blots were exposed to antibodies as described below and developed for chemiluminescence (SuperSignal Western; Pierce Biotechnology, Inc., Rockford, IL).

Immunoblot assays were performed by transient expression in COS cells in 10-cm dishes using DEAE dextran as described above. Cells were solubilized in immunoblot (IB) lysis buffer containing 0.15 M NaCl, 1% Triton X-100, 0.1% SDS, 1% sodium deoxycholate, 0.5 mM EDTA, 50 mM Tris-HCl, pH 7.5, 1 mM phenylmethylsulfonyl fluoride, and protease inhibitor cocktail (Roche). For GAL-4 or VP16 fusion proteins, cells were transferred to serum-free, phenol red-free medium containing 1 μM MG132, a proteosome inhibitor, 24 h after

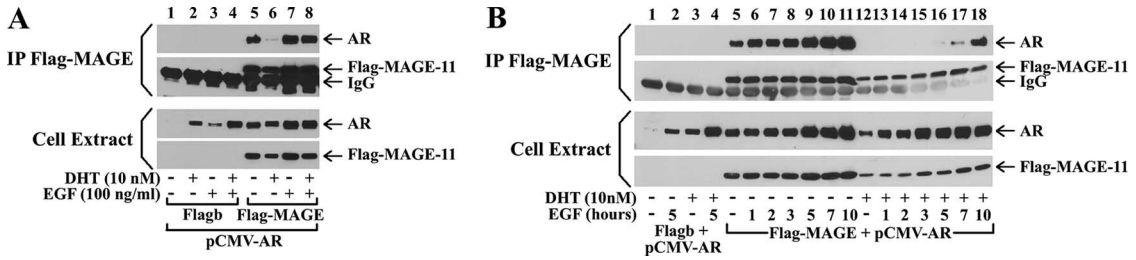

FIG. 1. EGF stabilizes the MAGE-AR-DHT complex. (A) COS cells were transfected with 2 μg pCMV-AR and 4 μg Flagb empty vector (lanes 1 to 4) or 2 μg pCMV-AR and 4 μg Flag-MAGE (lanes 5 to 8). Cells were treated with and without 10 nM DHT and 100 ng/ml EGF for 24 h as indicated. Fresh medium was added the next day and after 2.5 h. Cells were harvested, and protein extracts were prepared in IP lysis buffer for immunoprecipitation using anti-Flag affinity resin. Transfer blots of the immunoprecipitates (upper two panels) and cell extracts (8 μg protein/lane; lower two panels) were developed using AR32 and anti-Flag antibodies. (B) COS cells were transfected with 2 μg pCMV-AR and 5 μg Flagb (lanes 1 to 4) or 2 μg pCMV-AR and 5 μg Flag-MAGE (lanes 5 to 18) and 24 h later placed in serum-free, phenol red-free medium without hormone. The next day the medium was replaced with and without 10 nM DHT and 10 ng/ml EGF and incubated at 37°C from 1 to 10 h as indicated. Anti-Flag immunoprecipitates (upper two panels) and cell extracts (10 μg protein/lane; lower two panels) were prepared and assayed as for panel A.

transfection, fresh medium containing 1 μM MG132 was added the next day, and cells were harvested 1 h later. For siRNA experiments, COS cells (4×10^5/well in six-well plates) were transfected using Lipofectamine 2000 in DMEM without antibiotics with 0.5 μg pSG5-MAGE with and without 10 nM MAGE-11 siRNA, and cells were incubated for 48 h in serum-free, phenol red-free medium, harvested in PBS, and extracted in IB lysis buffer. Protein extracts were combined with 0.2 volumes of 6× sample buffer (10% SDS, 30% glycerol, 30% 2-mercaptoethanol, and 0.35 M Tris-HCl, pH 6.8), separated on 10 or 12% acrylamide gels containing SDS, and electrophoretically transferred to nitrocellulose membranes. Blots were probed as indicated using AR32 antipeptide antibody (rabbit polyclonal, 0.4 μg/ml) (48, 55), anti-Flag M2 monoclonal antibody (mouse monoclonal, 1:2,000 dilution; Sigma), HA-tag antibody (ab9110; rabbit polyclonal, 1:2,000 dilution; Abcam), rabbit anti-peptide MAGE-11 antibodies MagAb13-26 (3 or 4 μg/ml) and MagAb59-79 (3 or 4 μg/ml) (2), GAL-4 DNA binding domain antibody (sc-577; rabbit polyclonal, 1:500 dilution; Santa Cruz Biotechnology), VP16 activation domain antibody (sc-7546; mouse monoclonal, 1:100 dilution; Santa Cruz Biotechnology), phosphothreonine antibody (rabbit polyclonal, 1:1,000 dilution; Cell Signaling), and β-actin antibody (1:5,000 dilution; Abcam). MAGE-11 antibodies MagAb13-26 and MagAb59-79 were raised against MAGE-11 NH_2-terminal peptides and purified by peptide affinity chromatography (2). Data reported for all immunoprecipitation and immunoblot experiments are representative of two or more independent experiments.

Protein degradation rates. [^{35}S]methionine pulse-chase experiments were performed in COS cells in 10-cm dishes transfected using DEAE dextran as described elsewhere (21). Twenty-four h after transfection, cell cultures were placed in serum-free medium in the absence and presence of 10 ng/ml EGF. The next day, cells were washed in PBS and incubated in 4 ml methionine-free Dulbecco's modified Eagle's medium (Life Technologies, Inc.) containing 20 mM HEPES, pH 7.2 in the absence and presence of 10 ng/ml EGF. After 20 min at 37°C, 80 μCi [^{35}S]methionine (1,175 Ci/mmol; Easy Tag Express labeling mix; Perkin-Elmer) was added to each 10-cm dish, and cells were incubated for 30 min at 37°C. Cells were washed with PBS, and serum-free, phenol red-free, methionine-containing medium was added with and without 10 ng/ml EGF. At each time point, the medium was replaced on all plates and cells were harvested in 1 ml PBS after washing twice with PBS and sedimenting by centrifugation. Proteins were extracted in IB lysis buffer containing 1 mM dithiothreitol, 1 mM phenylmethylsulfonyl fluoride, and proteinase inhibitor cocktail (Sigma). Cells were sheared using a 1-ml pipetteman, incubated for 15 min at 4°C, and sedimented by centrifugation. The supernatant was combined with 8 μg MagAb13-26 and 10 μl protein A beads (Sigma). After 2 h of incubation at 4°C, beads were sedimented by centrifugation and washed twice in IB lysis buffer. Protein was solubilized in 50 μl 2× SDS sample buffer and analyzed on 10% acrylamide gels containing SDS. Proteins were transferred electrophoretically to nitrocellulose membranes and exposed to X-ray film. Autoradiographs were scanned and analyzed for optical density using an Image-Pro Plus spectrophotometer (Media Cybernetics, Silver Spring, MD).

Mass spectrometry. COS cells in 120 10-cm dishes (2×10^6 cells/dish) were transfected with 5 μg pSG5-MAGE/dish using DEAE dextran (21). Twenty-four h after transfection, cells were transferred to serum-free, phenol red-free medium containing 10 ng/ml EGF. The next day the medium was replaced and cells were harvested 2.5 h later in IP lysis buffer. MAGE-11 antibody MagAb13-26 purified on a peptide affinity column (3) was eluted in 25 mM sodium citrate-HCl, pH 2.5, and neutralized with 0.1 M sodium phosphate, pH 8.0. MAGE-11 protein was purified using 500 μg peptide purified MagAb13-26 antibody (3) coupled to 100 μl CNBr-activated Sepharose 4B (Amersham) according to the manufacturer's instructions and eluted in 10% ethanol and 10% formic acid for proteomic analysis by the Specialized Cooperative Centers Program in Reproduction and Infertility Research Proteomics Core of the UNC Chapel Hill—Duke Proteomics Center, Program in Molecular Biology and Bioinformatics.

In vitro kinase assay. Glutathione *S*-transferase (GST) fusion peptides GST-MAGE-^{354}EPKRLLTQN^{362}, GST-MAGE-^{354}EPKRLLAQN^{362} T360A mutant, and truncated human Cdc25C isoform A GST-^{210}GLYRSPSMPE^{219} Chk1 kinase substrate were expressed by cloning annealed oligos coding for the peptides into the EcoR1/Xho1 sites of pGEX-4T-1. For rapid insert verification, the 5′ oligo contained a 5′-AATTT end that disrupts the EcoR1 site after ligation. Fusion peptides were expressed in BL21-DE3 *E. coli* by inducing with 1 mM isopropyl-1-thio-β-D-galactopyranoside at 15°C overnight. Proteins were extracted from the pellet of a 100-ml culture using 4 ml GST extraction buffer (0.1 M NaCl, 1 mM EDTA, 0.5% NP-40, 20 mM Tris-HCl, pH 8.0, 1 mM phenylmethylsulfonyl fluoride, and proteinase inhibitor cocktail) by sonication and centrifugation. The bacterial lysate (0.5 ml) was combined with 10 μl GST-Sepharose 4B beads (Amersham Biosciences) and incubated for 2 h at 4°C. Beads were washed and suspended in 1.5 ml GST extraction buffer. Aliquots separated by gel electrophoresis were stained using GelCode Blue stain reagent (Pierce) to verify equivalent expression. Each of the GST-peptide–Sepharose bead suspensions (50 μl) was washed in Chk1 kinase buffer (1 mM EGTA, 0.4 mM EDTA, 5 mM $MgCl_2$, 0.05 mM DTT, and 5 mM morpholinepropanesulfonic acid, pH 7.2), pelleted with the ~10 μl kinase buffer remaining, and combined with 10 μl kinase buffer containing 1 μl full-length recombinant GST-Chk1 protein expressed from Sf9 cells (82 kDa; 0.1-mg/ml stock; specific activity, 369 nmol/min/mg; BioVision), 5 μl 0.25 mM cold ATP containing 0.16 μCi/μl [γ-^{32}P]ATP (10 mCi/ml, 3,000 Ci/mmol; Perkin-Elmer), and incubated at 30°C for 30 min. SDS sample buffer (6×; 7 μl) was added, and samples were boiled for 3 min and separated on a small 12% acrylamide gel containing SDS. The gel was dried under vacuum at 70°C for 1 h, exposed to X-ray film for 15 h, and then rehydrated in PBS and stained with brilliant blue R250 (Sigma) to verify equivalent protein loading.

RESULTS

EGF stabilizes the MAGE-AR-DHT complex. To investigate the transient nature of the AR and MAGE-11 complex in the presence of DHT, we determined the effects of EGF on the coimmunoprecipitation of AR with MAGE-11. Without EGF, AR coimmunoprecipitated with Flag-MAGE in the absence of DHT but was barely detected in the presence of DHT (Fig. 1A, top panel, lanes 5 and 6), as reported previously (3). However,

when cells were treated with EGF for 26 h, AR coimmunoprecipitated with MAGE-11 to a similar extent in the absence and presence of DHT (Fig. 1A, lanes 7 and 8). Immunoprecipitation of AR did not result from nonspecific aggregation, since AR was not detected in immunoprecipitates when using the Flag empty vector (Fig. 1A, lanes 1 to 4, and B, lanes 1 to 4). The low level of AR in cell extracts in the absence of DHT and MAGE-11 (Fig. 1A, third panel, lane 1) was detected after a longer film exposure (data not shown) and reflects the increase in AR degradation in the absence of MAGE-11 and without the stabilizing effect of the androgen-dependent AR N/C interaction (21, 35).

We found that the stabilizing influence of EGF on the MAGE-AR-DHT complex was time dependent, requiring 7 to 10 h of exposure of cells to EGF (Fig. 1B, top panel, lanes 12 to 18). In the absence of DHT, the levels of the MAGE-AR complex paralleled the levels of AR and MAGE-11 (Fig. 1B, lanes 5 to 11).

EGF and MAGE-11 regulate AR steady-state levels in the absence and presence of DHT. Immunoblots of protein extracted from cells treated in the absence of EGF without the coexpression of MAGE-11 showed higher levels of AR in the presence of increasing concentrations of DHT (Fig. 2A, top panel, lanes 1 to 8). This reflects the stabilizing effect of the androgen-dependent AR N/C interaction (21, 38, 62). However, DHT-bound AR levels were lower in the presence of EGF, suggesting EGF signaling interferes with the AR N/C interaction. With the coexpression of MAGE-11, AR levels increased overall but declined at 2 and 5 nM DHT in the absence and presence of EGF, with a further EGF-dependent decline at 10 nM DHT (Fig. 2A, lanes 11 to 18).

The decrease in AR in the presence of DHT with the coexpression of MAGE-11 appears to reflect the inhibitory effect of MAGE-11 on the AR N/C interaction (3), which was accentuated by EGF. The EGF-dependent lower level of AR at 10 nM DHT raised the possibility that EGF acting through MAGE-11 enhances the previously reported ability of MAGE-11 to increase AR turnover in the presence of DHT (3).

EGF increases MAGE-11 degradation in the presence of AR. To explore the mechanisms underlying EGF-dependent stabilization of the MAGE-AR complex, we determined the effects of EGF on MAGE-11 turnover in the presence of AR by immunoblotting and by [^{35}S]methionine pulse-chase analysis. When MAGE-11 was coexpressed with AR for 26 h in the presence of increasing concentrations of DHT, steady-state levels of MAGE-11 declined to the greatest extent in the presence of EGF at a saturating concentration of 10 nM DHT (Fig. 2A, second panel, lanes 9 to 18). [^{35}S]methionine pulse-labeling experiments performed in the absence of DHT indicated faster degradation rates of MAGE-11 in the presence of AR and EGF than with either AR or EGF alone (Fig. 2B). The half-life of MAGE-11 decreased from 5 to 6 h at 37°C in the presence of AR or EGF to 1.7 h with both AR and EGF (Fig. 2C).

The results suggest that the increased turnover of MAGE-11 accounts for the EGF- and AR-dependent decrease in MAGE-11 levels. Moreover, EGF-dependent stabilization of the MAGE-AR complex in the absence and presence of DHT (Fig. 1A) occurs in association with the increased turnover of AR and MAGE-11.

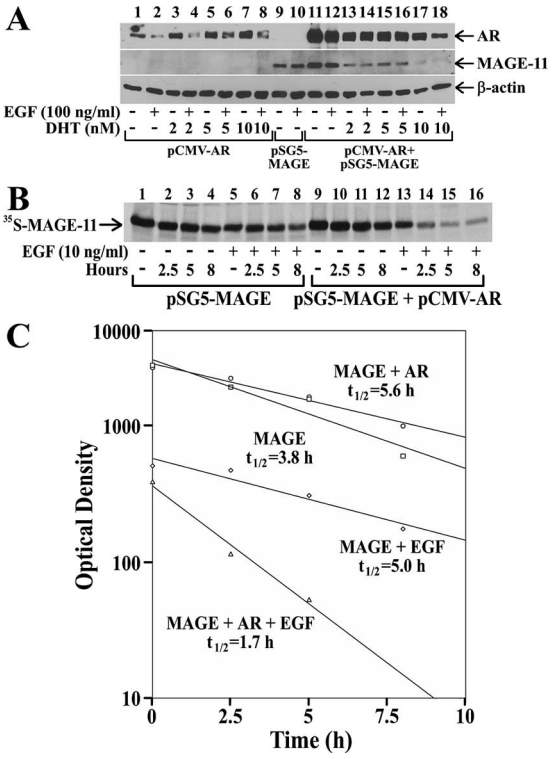

FIG. 2. EGF regulates the turnover of AR and MAGE-11. (A) COS cells were transfected with 4 μg pCMV-AR (lanes 1 to 8), 4 μg pSG5-MAGE (lanes 9 and 10), and 4 μg pCMV-AR with 4 μg pSG5-MAGE (lanes 11 to 18). Cells were treated 24 h after transfection with and without 2, 5, and 10 nM DHT in the absence and presence of 100 ng/ml EGF as indicated. Cells were harvested 48 h later in IB lysis buffer and analyzed (10 μg protein/lane) on a 10% acrylamide gel containing SDS. The transfer blot was probed with AR32, MagAb13-26, and β-actin antibodies as indicated. (B) COS cells were transfected with 2 μg pSG5-MAGE without (lanes 1 to 8) and with 2 μg pCMV-AR (lanes 9 to 16). Twenty-four h after transfection, cells were placed in serum-free, phenol red-free medium in the absence (lanes 1 to 4 and 9 to 12) and presence (lanes 5 to 8 and 13 to 16) of 10 ng/ml EGF. The next day cells were placed in methionine-free medium with or without EGF and incubated for 30 min with [^{35}S]methionine. The medium was replaced with serum-free, methionine-containing medium with and without EGF, and cells were harvested at 0, 2.5, 5, and 8 h. Cell extracts containing 0.35 mg protein were immunoprecipitated using MagAb13-26, and the transfer blot was exposed to X-ray film. (C) Quantitation of ^{35}S labeling. The autoradiograph in panel B was scanned using an Image Pro Plus spectrophotometer, and the data are plotted on a semilog scale.

EGF enhances the ubiquitinylation of MAGE-11. The increase in MAGE-11 turnover in the presence of AR and EGF raised the possibility that EGF modulates the MAGE-AR complex through the ubiquitinylation of MAGE-11. This hypothesis was supported by the results of immunoblot assays performed in the absence and presence of AR and probed with a MAGE-11-specific antibody. In addition to the major ~70-kDa MAGE-11 band detected without the coexpression of AR, EGF caused the appearance of a weaker ~80-kDa band that was not present after EGF treatment in the absence of MAGE-11 (Fig. 3A, lanes 1 to 4). A ~130-kDa immunoreac-

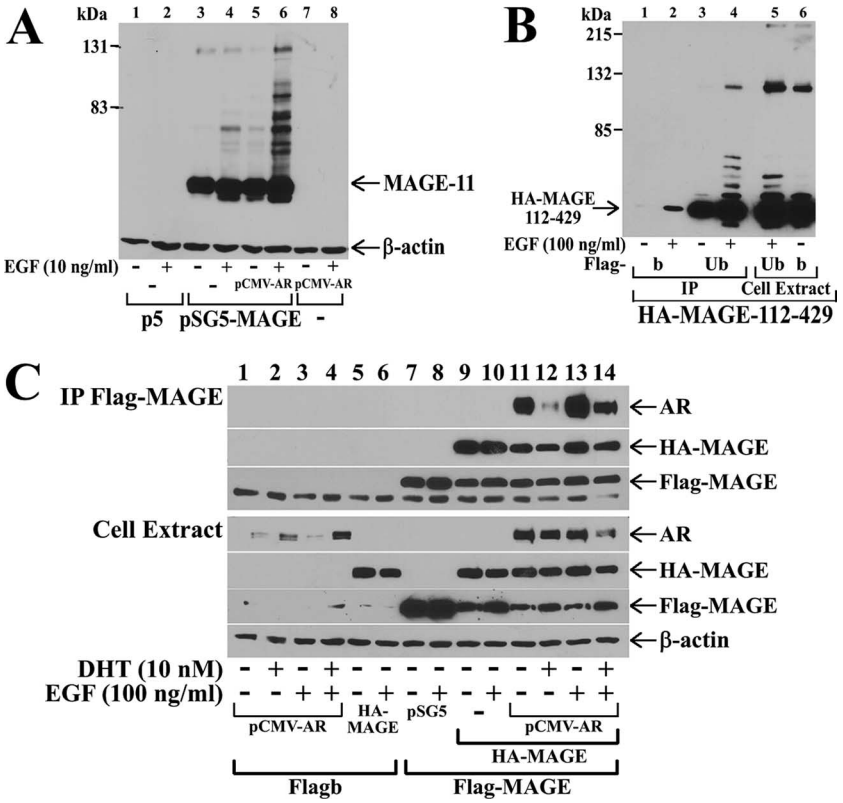

FIG. 3. MAGE-11 ubiquitinylation and dimerization. (A) Effects of EGF and AR on MAGE-11 ubiquitinylation. COS cells were transfected with 2 μg pSG5 empty vector (p5, lanes 1 and 2), 2 μg pSG5-MAGE in the absence (lanes 3 and 4) or presence (lanes 5 and 6) of 2 μg pCMV-AR, and 2 μg pCMV-AR alone (lanes 7 and 8) and treated 24 h later with and without 10 ng/ml EGF as indicated. The next day the medium was replaced with fresh medium with or without EGF. Cell extracts were prepared 2 h later in IB lysis buffer and analyzed (50 μg/lane) on a 10% acrylamide gel. The transfer blot was probed using MagAb59-79 antibody. (B) EGF-induced ubiquitinylation of MAGE-11. COS cells were transfected with 6 μg Flagb empty vector and 3 μg pSG5-HA-MAGE-112-429 (lanes 1, 2, and 6) or 6 μg FlagUb and 3 μg pSG5-HA-MAGE-112-429 (lanes 3 to 5) and treated 24 h later in the absence (lanes 1, 3, and 6) or presence (lanes 2, 4, and 5) of 100 ng/ml EGF. The next day, protein extracts were prepared in IP lysis buffer, and anti-Flag resin was used to immunoprecipitate FlagUb. Shown are immunoprecipitated proteins (IP; lanes 1 to 4) and cell extracts (25 μg protein/lane; lanes 5 and 6). The transfer blot was probed using HA tag antibody. (C) EGF- and AR-independent dimerization of MAGE-11. COS cells were transfected with 4 μg Flag-b and 2 μg pCMV-AR (lanes 1 to 4), 4 μg Flagb and 2 μg pSG5-HA-MAGE (lanes 5 and 6), 4 μg Flag-MAGE and 2 μg pSG5 (lanes 7 and 8), 4 μg Flag-MAGE and 2 μg pSG5-HA-MAGE (lanes 9 and 10), and 4 μg Flag-MAGE, 2 μg pCMV-AR, and 2 μg pSG5-HA-MAGE-11 (lanes 11 to 14). Cells were treated 24 h later with and without 10 nM DHT and 100 ng/ml EGF as indicated. The next day the media were exchanged, and 2 h later cells were harvested in IP lysis buffer and protein extracts were immunoprecipitated using anti-Flag M2 affinity gel. Immunoprecipitates (upper three panels) and cell lysates (10 μg protein/lane; lower four panels) were analyzed on 10% acrylamide gels containing SDS, and the transfer blots were probed using AR32, HA, Flag, and β-actin antibodies as indicated.

tive MAGE-11 band was also detected in the absence and presence of EGF (Fig. 3A, lanes 3 and 4), and there was a slightly faster migrating minor band, possibly resulting from partial degradation.

With the coexpression of AR, the 80- and 130-kDa forms of MAGE-11 were barely detected in the absence of EGF (Fig. 3A, lane 5). However, in the presence of AR and EGF, a ladder of more intense higher-molecular-mass bands that included the EGF-induced 80-kDa band seen in the absence of AR was evident with the MAGE-11 antibody (Fig. 3A, lanes 4 and 6). Absence of the slower migrating protein bands when AR was expressed by itself (Fig. 3A, lanes 7 and 8) provided further evidence that the protein bands represent modified forms of MAGE-11.

To determine whether the slower migrating immunoreactive forms of MAGE-11 resulted from ubiquitinylation, we coexpressed Flag-tagged ubiquitin with HA-MAGE-112-429, an HA-tagged carboxyl-terminal fragment of MAGE-11 that interacts with AR (3). In the absence and presence of EGF, ubiquitinylated forms of MAGE-11 were suggested by the Flag-Ub immunoprecipitates and cell extracts detected using an HA tag antibody (Fig. 3B, lanes 3 to 6). After treatment with EGF, an additional ladder of slower migrating MAGE-11 bands coimmunoprecipitated with Flag-Ub and was present in the cell extract (Fig. 3B, lanes 4 and 5).

The ~130-kDa band evident in the cell extracts and immunoprecipitates (Fig. 3A and B) appeared to represent a MAGE-11 homodimer that persisted after reducing denaturation and analysis in SDS-containing gels. Immunoprecipitation of the MAGE-11 dimer by the Flag antibody after coexpression with Flag-Ub indicated that the dimer was also likely ubiquitinylated in response to EGF (Fig. 3B, lanes 3 and 4). Dimerization of MAGE-11 was supported by experiments where we coexpressed Flag-MAGE with pSG5-HA-MAGE.

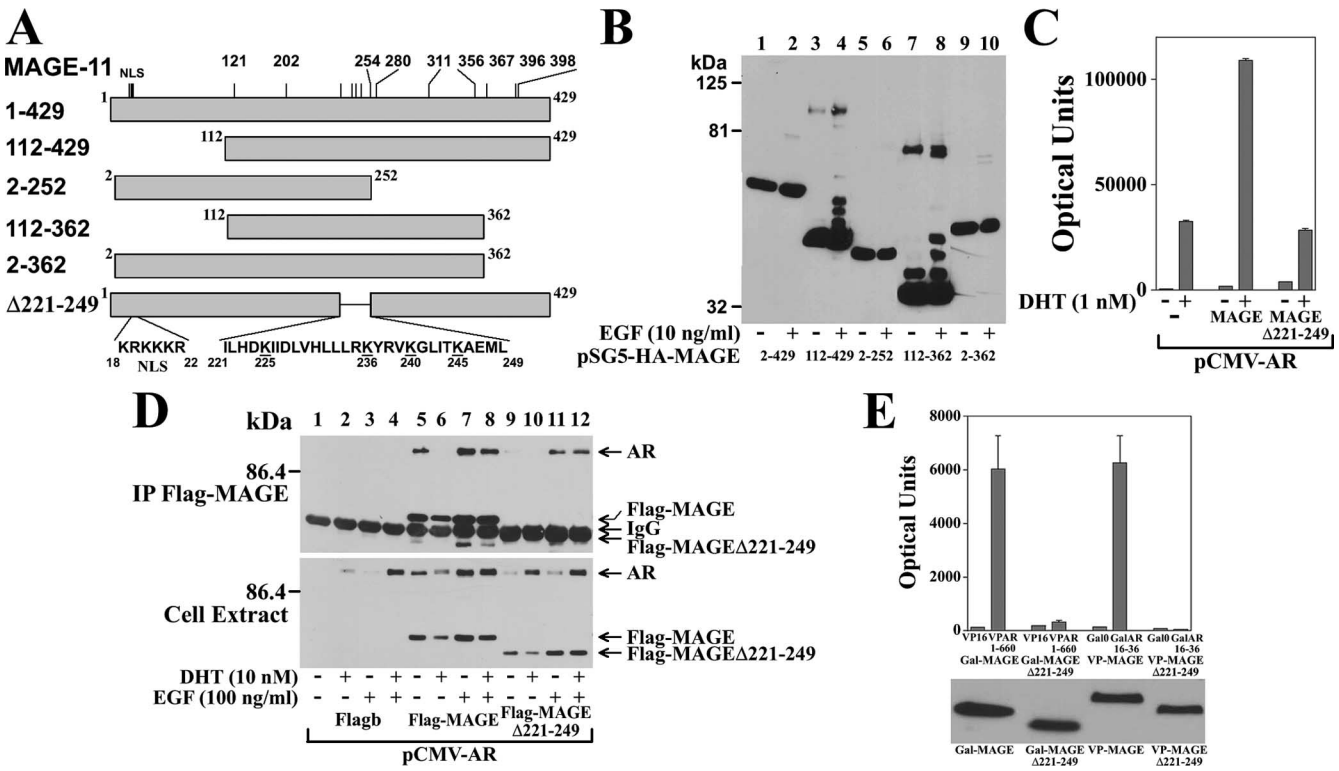

FIG. 4. Region of ubiquitinylation in MAGE-11. (A) Schematic diagram of full-length MAGE-11 (amino acid residues 1 to 429) and fragments. The amino acid sequence is shown for the MAGE-11 nuclear localization signal (NLS; residues 18 to 22) and the amino acid 221 to 249 region that contains Lys-225, -236, -240, and -245. (B) Ubiquitinylation in the central region of MAGE-11. COS cells were transfected with 5 μg pSG5-HA-MAGE-2-429 (lanes 1 and 2), 1 μg pSG5-HA-MAGE-112-429 (lanes 3 and 4), 5 μg pSG5-HA-MAGE-2-252 (lanes 5 and 6), 1 μg pSG5-HA-MAGE-112-362 (lanes 7 and 8), or 5 μg pSG5-HA-MAGE-2-362 (lanes 9 and 10) and 24 h later treated in the absence or presence of 10 ng/ml EGF as indicated. The next day the media with and without EGF were replaced and again incubated for 2.5 h. After the second 2.5-h incubation, protein extracts were prepared in IB lysis buffer containing 50 mM NaF and phosphatase inhibitor cocktail 1 and 2 (Sigma) and analyzed (15 to 25 μg/lane) by immunoblotting using HA tag antibody. (C) Loss of the MAGE-11-dependent increase in AR transcriptional activity by MAGEΔ221-249. CV1 cells were transfected with 5 μg PSA-Enh-Luc and 0.1 μg pCMV-AR with and without 2 μg pSG5-MAGE and 2 μg pSG5-MAGEΔ221-249 as indicated. Cells were incubated in the absence and presence of 1 nM DHT for 48 h, and luciferase activity was determined. (D) Reduced interaction between AR and MAGEΔ221-249. COS cells were transfected with 2 μg pCMV-AR in the presence of 4 μg Flagb empty vector (lanes 1 to 4), 4 μg Flag-MAGE (lanes 5 to 8), and 4 μg Flag-MAGEΔ221-249 (lanes 9 to 12) and 24 h later cultured in the absence and presence of 10 nM DHT and 100 ng/ml EGF as indicated. The next day the media were replaced and cells were incubated an additional 2.5 h. Cells were extracted in IP lysis buffer and immunoprecipitated using anti-Flag affinity resin. Shown are immunoblots of immunoprecipitates (upper panel) and cell extracts (8 μg/lane; lower panel) probed with AR32 and anti-Flag antibodies. (E) Loss of AR interaction with MAGEΔ221-249. Luciferase activity was determined in two-hybrid assays using HeLa cells transfected with 0.1 μg 5XGAL4Luc3 and 0.05 μg GAL-MAGE or GAL-MAGEΔ221-249 with 0.05 μg VP16 or VP-AR1-660 as indicated and with 0.05 μg VP-MAGE or VP-MAGEΔ221-249 with 0.05 μg GAL-0 or GAL-AR16-36 as indicated. In the lower panel, immunoblots of extracts from COS cells transfected with 10 μg GAL-MAGE, GAL-MAGEΔ 221-249, VP-MAGE, and VP-MAGEΔ221-249 are shown. After 24 h cells were placed in medium containing 1 μM MG132, a proteosome inhibitor which was readded in fresh medium the next day, and cells were harvested 1 h later. Protein extracts in IB lysis buffer (60 μg protein/lane) were separated on a 12% acrylamide gel containing SDS. Transfer blots were probed with GAL-4 (left two lanes) and VP16 antibodies (right two lanes).

HA-MAGE-11 coimmunoprecipitated with Flag-MAGE in the absence and presence of AR and EGF (Fig. 3C, upper panels, lanes 9 to 14). The DHT- and EGF-dependent coimmunoprecipitation of AR with Flag-MAGE-11 (Fig. 3C, upper panel, lanes 11 to 14) was similar to that seen in Fig. 1A and did not result from an effect of EGF on MAGE-11 dimerization.

The results suggest that EGF increases the ubiquitinylation of MAGE-11 in association with stabilization of the AR-MAGE complex independent of an effect on MAGE-11 dimerization.

Region of ubiquitinylation in MAGE-11. To localize the region in MAGE-11 that harbors EGF-dependent ubiquitinylation sites, we expressed a series of HA-MAGE fragments, shown schematically in Fig. 4A. Using an HA tag antibody, we found that the carboxyl-terminal MAGE-112-429 fragment and central fragment MAGE-112-362 exhibited EGF-dependent ladders of slower migrating bands (Fig. 4B). There was also a slower migrating band less dependent on EGF, indicative of MAGE-11 dimerization. In contrast, MAGE-2-429 and NH_2-terminal fragments 2–362 and 2–252 each had an EGF-dependent slower migrating band similar in intensity and mobility shift to the 80-kDa form of MAGE-11 seen with full-length 70-kDa MAGE-11 (Fig. 3A). The dimer band not apparent with the NH_2-terminal fragments of MAGE-11 (Fig. 4B) was detected on longer exposure of the film (data not shown).

The presence of four potential lysine ubiquitinylation sites

(Fig. 4A) within the α-helical region between amino acids 221 and 249 predicted by PONDR plot (http://www.pondr.com) prompted us to test MAGEΔ221-249 for its ability to interact with AR. We found that Flag-MAGEΔ221-249 did not stabilize AR in cell extracts in the absence of DHT (Fig. 4D, lower panel). Moreover, coimmunoprecipitation of AR with Flag-MAGEΔ221-249 decreased relative to full-length Flag-MAGE in the absence and presence of EGF (Fig. 4D, upper panel), and MAGEΔ221-249 did not increase AR transcriptional activity (Fig. 4C). Loss of the AR coregulatory function of MAGE-11 by MAGEΔ221-249 appears to result from its inability to bind the AR FXXLF motif. Two-hybrid interaction assays using VP16 and GAL-4 fusion proteins demonstrated that MAGEΔ221-249 did not interact with the AR NH_2-terminal FXXLF motif-containing fragments AR1-660 and AR16-36 (Fig. 4E, upper panel) under conditions where MAGEΔ221-249 mutant expression levels were similar to the wild type (Fig. 4E, lower panel).

The results raised the possibility that EGF-dependent ubiquitinylation sites among the lysine residues in the amino acid 221 to 249 region are required for MAGE-11 to interact with AR. The data suggested in addition that when MAGE-11 is not bound to AR, the MAGE-11 NH_2-terminal region has an inhibitory effect on EGF-dependent ubiquitinylation of MAGE-11.

Identification and functional effects of site-specific ubiquitinylation in MAGE-11. To identify the ubiquitinylation sites in MAGE-11, we prepared a series of lysine-to-alanine mutants in full-length MAGE-11 and tested their ability to increase AR transcriptional activity in the absence and presence of transcriptional intermediary factor 2 (TIF2), an SRC/p160 coactivator that increases AR transcriptional activity (22, 24). MAGE-K225A and -K236A increased AR transcriptional activity similar to wild-type MAGE-11 in the absence and presence of coexpressed TIF2 (Fig. 5A). In contrast, MAGE-K240A, -K245A, and the double and multiple lysine mutants lost most of the stimulatory effect of MAGE-11 on AR transcriptional activity in the absence or presence of TIF2 but expressed at levels similar to the wild type (Fig. 5A, lower panel).

The requirements for MAGE-11 ubiquitinylation in modulating AR transcriptional activity were further evaluated by testing the effects of the lysine mutants on AR AF2 activity in the carboxyl-terminal region and AF1 activity in the NH_2-terminal region. To measure AF2 transcriptional activity, we coexpressed TIF2 with ARΔ120–472, an AR deletion mutant that lacks the NH_2-terminal AF1 region but retains the NH_2-terminal FXXLF motif region required for the AR N/C interaction and for MAGE-11 to interact with AR. We found that the transcriptional activity of ARΔ120–472 depends on the coexpression of MAGE-11 and TIF2 (Fig. 5B). This reflects the ability of MAGE-11 to bind the AR FXXLF motif and relieve inhibition of AF2 recruitment of SRC/p160 coactivators caused by the AR N/C interaction (1, 3, 21). MAGE-K240A and -K245A did not activate ARΔ120–472 in the presence of coexpressed TIF2, whereas MAGE-K225A and -K236A retained the activity of wild-type MAGE-11.

We found that the MAGE-11-dependent increase in AR AF1 activity also depended on MAGE-11 residues Lys-240 and Lys-245. The constitutive activity of AR1-660, an AR NH_2-terminal and DNA binding domain fragment assayed in the absence of TIF2, increased with the coexpression of MAGE-11 (Fig. 5C). However, MAGE-K240A and -K245A were less effective than wild-type MAGE-11 and the K236A mutant in increasing AR AF1 activity. The coregulatory function of MAGE-11 was abolished by the triple mutation K236A,K240A, K245A.

Two-hybrid interaction assays demonstrated that the inabilities of MAGE-K240A and -K245A to increase AR transcriptional activity resulted from ineffective binding of MAGE-11 to the AR FXXLF motif. The GAL-4 and VP16 fusion proteins of the MAGE-11 lysine-to-alanine mutants' expression levels were similar to the wild type but lost to varying degrees the ability to interact with the AR FXXLF motif-containing fragments VP-AR1-660 and GAL-AR16-36 (Fig. 5D). MAGE-K240A, MAGE-K245A, and the multiple site mutants showed the greatest loss of binding to AR, providing further evidence that Lys-240 and Lys-245, and possibly Lys-236, are required for MAGE-11 to interact with AR and increase AR transcriptional activity.

The results suggest that EGF-dependent ubiquitinylation of MAGE-11 at Lys-240 and Lys-245 is required for MAGE-11 to increase AR transcriptional activity.

Dependence of the AR-MAGE interaction on ubiquitinylation. To establish whether the EGF-dependent ubiquitinylation of MAGE-11 occurs at the same lysine residues required for MAGE-11 to bind AR, we tested the effect of the lysine mutations on the EGF-dependent stabilization of the AR-MAGE complex and the appearance of the slower migrating forms of MAGE-11. We found that AR levels were lower in the presence of MAGE-K240A compared to wild-type MAGE-11 in extracts from cells treated in the absence or presence of EGF (Fig. 6A, third panel, lanes 13 to 16). Moreover, coimmunoprecipitation of MAGE-11 and AR was diminished by the K240A mutation (Fig. 6A, upper panel, lanes 13 to 16) to a similar extent as the K245A (data not shown) and K225A,K236A,K240A,K245A mutations (Fig. 6A, upper panel, lanes 9 to 12). EGF-dependent immunoprecipitation of the slower migrating forms of MAGE-112-429 and the -K236A mutant was almost eliminated by the single K240A and K245A or multiple K236A,K240A,K245A mutations (Fig. 6B, lower panel), even though expression levels were similar (Fig. 6B, upper panel).

Multiple ubiquitinylated forms of MAGE-11 could result from polyubiquitinylation of MAGE-bound ubiquitin or multiple monoubiquitinylation of MAGE-11. To test this, we performed experiments using lysine-free Flag-Ub-KO, in which all ubiquitin lysine residues were mutated to arginine in order to prevent polyubiquitinylation of MAGE-bound ubiquitin. We found that ubiquitinylated forms of MAGE-11 persisted when we used lysine-free ubiquitin, although there was a change in the migration pattern (Fig. 6C, lanes 3 to 6), suggesting both mono- and polyubiquitinylation of MAGE-11. However, we found that AR coimmunoprecipitated to a similar extent as wild type and lysine-free Flag-Ub in a DHT- and EGF-dependent manner that required the presence of MAGE-11 (Fig. 6C, lanes 7 to 18). Coimmunoprecipitation of AR with Flag-Ub in the presence of HA-MAGE-112-429 (Fig. 6D, lanes 3 to 12) did not occur in the presence of HA-MAGE-112-429-K236A,K240A,K245A (Fig. 6D, lanes 13 to 16, 3KA).

The results suggest that EGF enhances mono- and poly-

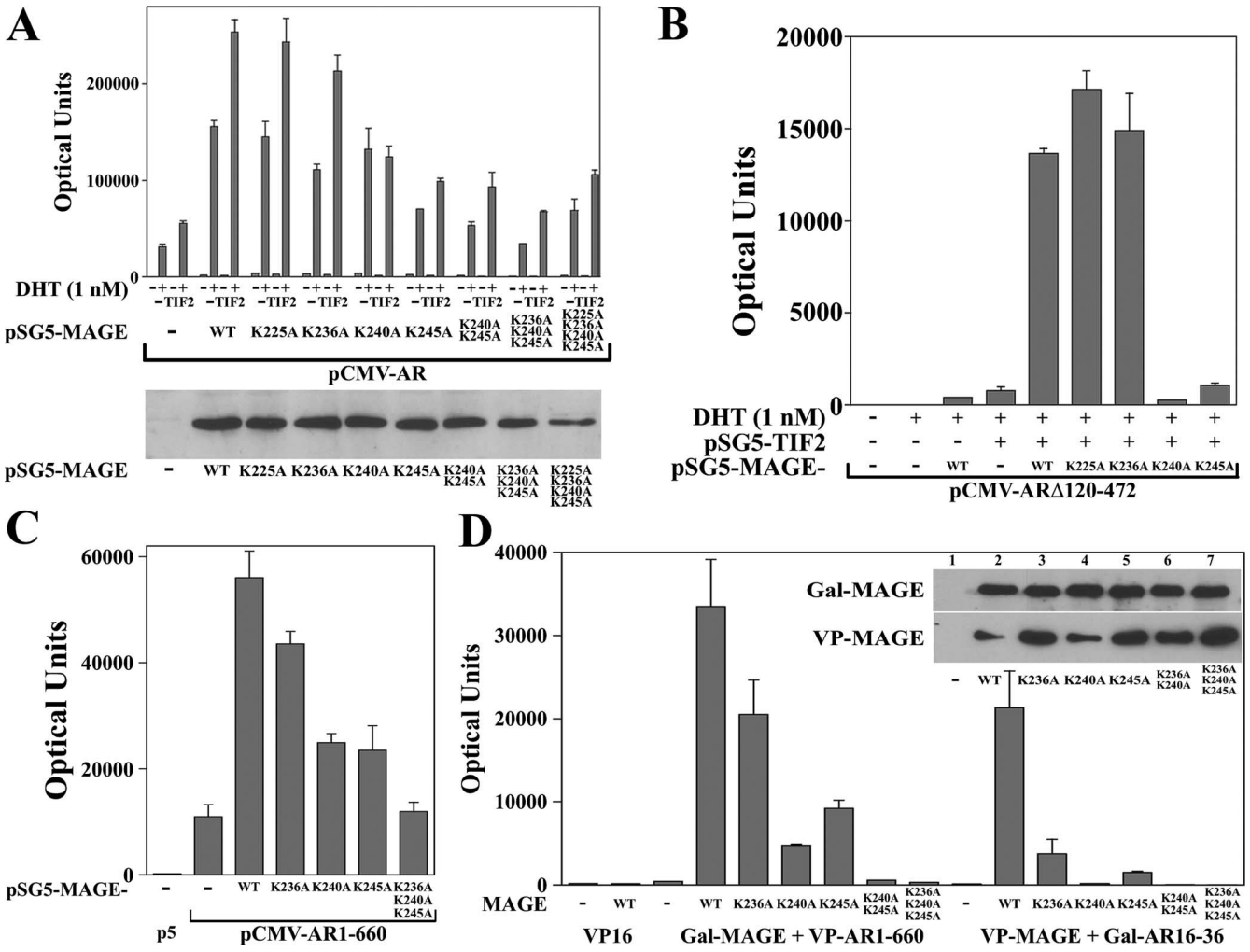

FIG. 5. Inhibition of MAGE-11 coregulator function by lysine mutations. (A) Decreased AR transcriptional activity by MAGE-11 lysine mutants. CV1 cells were transfected with 5 μg PSA-Enh-Luc and 0.1 μg pCMV-AR in the absence and presence of 2 μg pSG5-TIF2 and 2 μg pSG5-MAGE wild-type (WT) and the indicated lysine-to-alanine mutants. Cells were incubated for 48 h in the absence and presence of 1 nM DHT, and luciferase activity was measured. The lower panel shows immunoblot results with cell extracts from COS cells transfected with 4 μg pSG5 empty vector (−), wild-type (WT) pSG5-MAGE, or the indicated lysine-to-alanine mutants. Protein extracts (20 μg/lane) were separated on a 10% gel, and the transfer blot was probed with MagAb13-26 antibody. (B) Inability of MAGE-K240A and MAGE-K245A to increase AR AF2 activity. CV1 cells were transfected with 5 μg MMTV-Luc, 0.1 μg pCMV-ARΔ120–472 (with a deletion of the AR NH_2-terminal AF1 region) with 2 μg WT pSG5-MAGE alone, 2 μg pSG5-TIF2 alone, and 2 μg pSG5-TIF2 with 2 μg WT pSG5-MAGE and K225A, K236A, K240A and K245A mutants as indicated. Cells were incubated for 48 h in the absence and presence of 1 nM DHT, and luciferase activity was measured. (C) Effects of MAGE-11 lysine mutants on AR AF1 constitutive activity. HeLa cells were transfected with 0.1 μg PSA-Enh-Luc and 0.01 μg pCMV-AR1-660 in the absence and presence of 0.1 μg WT pSG5-MAGE and K236A, K240A, K245A, and K236A,K240A,K245A mutants as indicated. Cells were incubated for 48 h before measuring luciferase activity. (D) Two-hybrid interaction between AR and MAGE-11 lysine mutants. HeLa cells were transfected with 0.25 μg 5XGAL4Luc3 and 0.05 μg WT or the indicated lysine-to-alanine mutant in GAL-MAGE or VP-MAGE with 0.05 μg VP-AR1-660 or GAL-AR16-36. The next day cells were incubated for 48 h before measuring luciferase activity. (Inset) immunoblots of extracts from COS cells transfected with 8 μg GAL-0 (−) and WT and mutant GAL-MAGE (top panel) and pVP16 (−) and WT and mutant VP-MAGE (bottom panel), as indicated. After 24 h, cells were transferred to medium containing 1 μM MG132, which was readded in fresh medium the next day and cells were harvested 1 h later. Protein extracts in IB lysis buffer (50 μg/lane) were separated on 10% acrylamide gels containing SDS. Transfer blots were probed using GAL-4 (upper panel) and VP16 (lower panel) antibodies.

ubiquitinylation of MAGE-11 at sites that include lysine residues 240 and 245 and that multiple monoubiquitinylation of MAGE-11 is required for the formation of the AR-MAGE complex. Absence of AR in the coimmunoprecipitates without the coexpression of MAGE-11 (Fig. 6C, lanes 7 to 10, and D, lanes 3 to 6) indicated that AR was not ubiquitinylated under the assay conditions.

Phosphorylation of MAGE-11. EGF signaling influences transcriptional events through protein phosphorylation. We therefore sought to identify the phosphorylation sites in MAGE-11 that influence EGF-dependent ubiquitinylation of MAGE-11 and its ability to increase AR transcriptional activity. Gel migration profiles were compared between wild-type HA-MAGE-112-362 and with single and multiple serine-to-

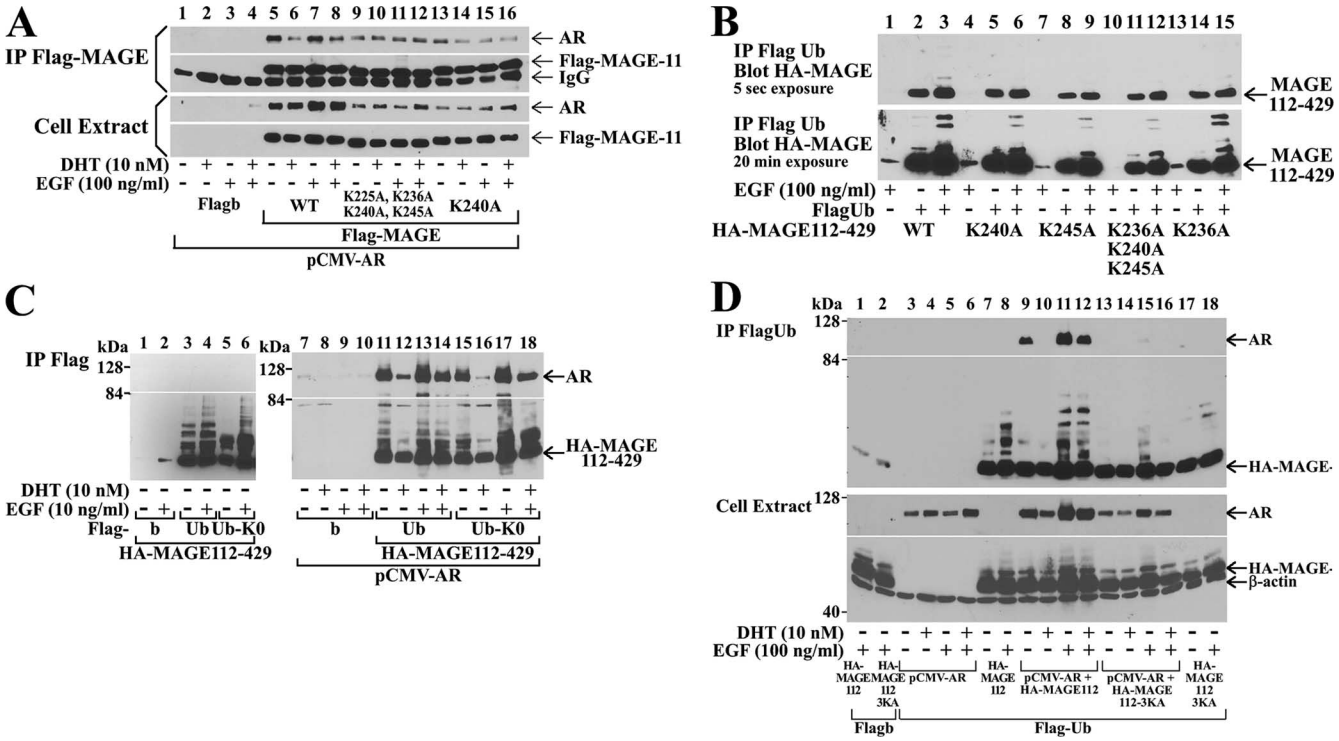

FIG. 6. Requirement of MAGE-11 ubiquitinylation to interact with AR. (A) COS cells were transfected with 1 μg pCMV-AR in the presence of 4 μg Flagb empty vector (lanes 1 to 4), wild-type (WT) Flag-MAGE (lanes 5 to 8), Flag-MAGE-K225A,K236A,K240A,K245A (lanes 9 to 12), or Flag-MAGE-K240A (lanes 13 to 16). Cells were treated 24 h later in the absence and presence of 10 nM DHT and 100 ng/ml EGF as indicated. The next day media were replaced and cells were incubated for 2 h at 37°C. Flag-MAGE was immunoprecipitated using anti-Flag M2 affinity resin, and the immunoprecipitates (upper two panels) and cell extracts (10 μg/lane; lower two panels) were separated on 10% acrylamide gels. Transfer blots were probed using AR32 and anti-Flag M2 monoclonal antibodies. (B) COS cells were transfected with 6 μg Flagb (lanes 1, 4, 7, 10, and 13) (−) and 6 μg FlagUb as indicated with 2 μg WT pSG5-HA-MAGE-112-429 and the indicated lysine-to-alanine mutants. After 24 h cells were treated in the absence and presence of 100 ng/ml EGF as indicated. Cells were harvested the next day, and protein extracts were immunoprecipitated using anti-Flag M2 affinity resin. Immunoprecipitates were separated on 10% acrylamide gels containing SDS. Transfer blots were probed for MAGE-11 using HA tag antibody. X-ray film was exposed for 5 s (upper panel) and 20 min (lower panel). (C) In the left panel, COS cells were transfected with 3 μg pSG5-HA-MAGE-112-429 together with 6 μg Flagb (lanes 1 and 2), 6 μg Flag-Ub (lanes 3 and 4), and 6 μg Flag-Ub-KO, in which all ubiquitin lysine residues were changed to arginine (lanes 5 and 6). In the right panels, COS cells were transfected with 2 μg pCMV-AR together with 6 μg Flagb (lanes 7 to 10), 6 μg Flag-Ub and 3 μg pSG5-HA-MAGE-112-429 (lanes 11 to 14), and 6 μg Flag-Ub-KO and 3 μg pSG5-HA-MAGE-112-429 (lanes 15 to 18). Cells were incubated for 24 h in the absence and presence of 10 nM DHT and 10 ng/ml EGF as indicated, and extracts were prepared in IB (lanes 1 to 6) and IP (lanes 7 to 18) lysis buffer and analyzed by immunoblotting with AR32 and HA tag antibodies. (D) COS cells were transfected with 6 μg Flagb and 3 μg pSG5-HA-MAGE-112-429 (lane 1), 6 μg Flagb and 3 μg pSG5-HA-MAGE-112-429-K236A,K240A,K245A (HA-MAGE-112-3KA, lane 2), 6 μg Flag-Ub and 2 μg pCMV-AR (lanes 3 to 6), 6 μg Flag-Ub and 3 μg pSG5-HA-MAGE-112-429 in the absence (lanes 7 and 8) and presence (lanes 9 to 12) of 2 μg pCMV-AR, and 6 μg Flag-Ub with 3 μg pSG5-HA-MAGE-112-429-K236A,K240A,K245A (HA-MAGE-112-3KA) in the presence (lanes 13 to 16) and absence (lanes 17 and 18) of 2 μg pCMV-AR. Cells were incubated for 24 h in the absence and presence of 10 nM DHT and 100 ng/ml EGF as indicated and extracted in IP lysis buffer. The blots were probed with AR32, HA, and β-actin antibodies as indicated.

alanine mutations at consensus phosphorylation sites. Extracts from EGF-treated cells were analyzed with and without treatment with λ-phosphatase.

We found that EGF increased, and λ-phosphatase slowed, the electrophoretic mobility of MAGE-112-362 and its EGF-induced ubiquitinylated forms (Fig. 7A, top panel, lanes 1 to 3, and lower panel, lanes 16 and 17), suggesting the changes in gel migration are indicative of phosphorylation. Phosphatase treatment slowed the migration of MAGE-112-362 with individual mutations at predicted consensus phosphorylation sites Ser-174, Ser-181, and Ser-208 but had less of an effect on the S174A,S181A,S208A triple mutant (Fig. 7A, upper panel). In contrast, migration of MAGE-112-362 with simultaneous mutations at Ser-168, -170, -174, -181, -199, and -208 was unaltered by EGF with or without phosphatase treatment (Fig. 7A, lower panel, lanes 23 to 25).

The results suggest that EGF-dependent phosphorylation of MAGE-11 occurs among serine residues 168, 170, 174, 181, 199, and 208. Phosphorylation at Ser-208 was confirmed by mass spectrometry (data not shown). However, none of these single or multiple serine mutations diminished the ability of full-length MAGE-11 to increase AR transcriptional activity, as shown for the six-serine mutant (Fig. 7B, 6-SA). In addition, the greater intensity of the slower migrating ubiquitinylated forms of the serine-to-alanine MAGE-11 mutants observed after treatment with EGF (Fig. 7A) indicated that serine phosphorylation among these sites does not influence the EGF-dependent ubiquitinylation of MAGE-11.

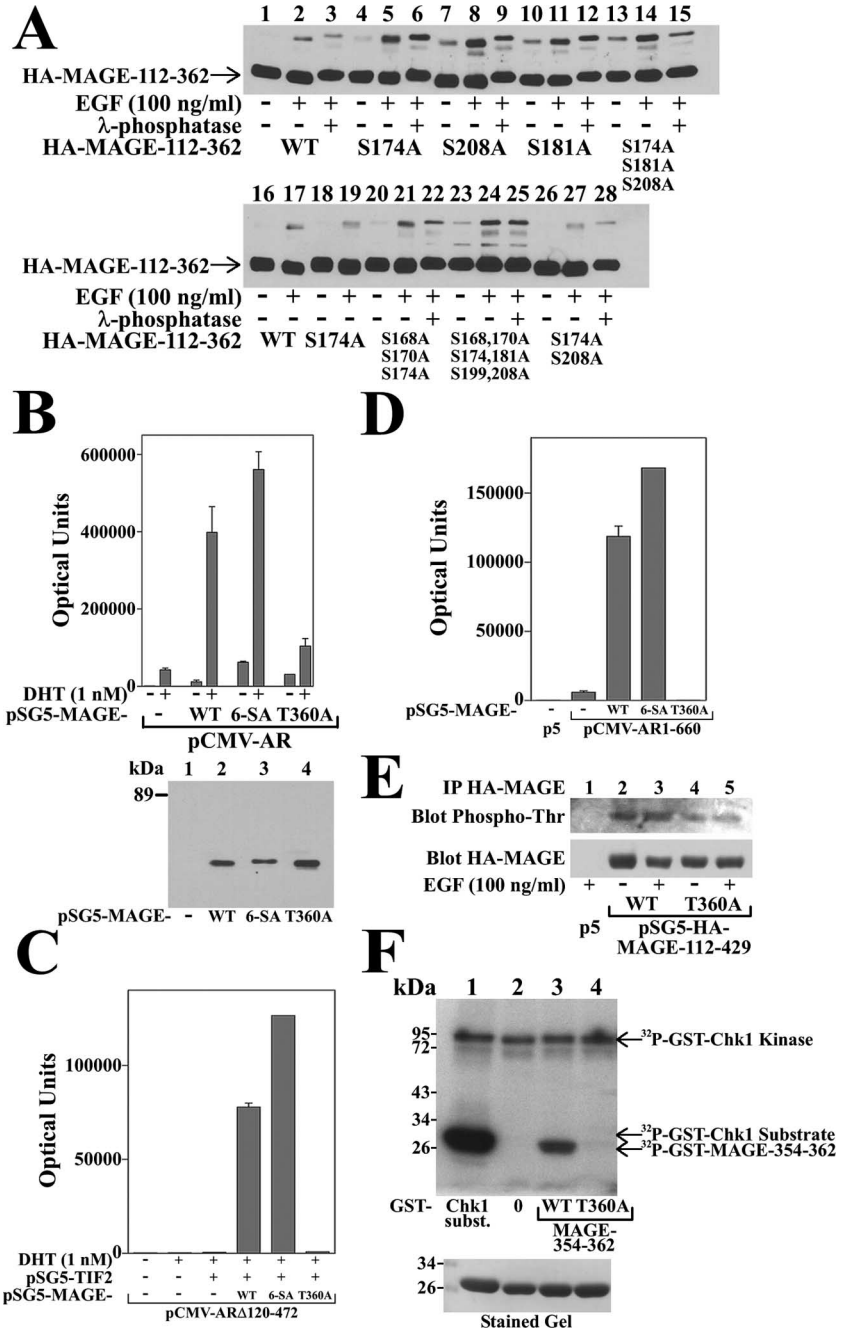

FIG. 7. Phosphorylation sites in MAGE-11. (A) Effects of λ-phosphatase on the electrophoretic mobility of MAGE-11 serine mutants. COS cells were transfected with 2 μg wild-type (WT) pSG5-HA-MAGE-112-362 and with the indicated serine-to-alanine mutants. The next day cells were incubated for 24 h in the absence and presence of 100 ng/ml EGF as indicated. Media with and without EGF were replaced and cells were incubated an additional 2 h at 37°C and harvested in 0.2 ml IP lysis buffer without sodium fluoride. Protein extracts (2 μg) from EGF-treated cells were incubated in 40 μl for 1 h at 4°C with and without 400 IU λ-phosphatase (New England Biolabs). Samples were analyzed on 12% acrylamide gels containing SDS, and transfer blots were probed with HA tag antibody. Shown are the major (arrow) and slower-migrating ubiquitinylated forms of WT and mutant HA-MAGE-112-362. (B) MAGE-T360A lacks coactivator activity. CV1 cells were transfected with 5 μg PSA-Enh-Luc and 0.1 μg pCMV-hAR with and without 1 μg WT pSG5-MAGE and the S168A,S170A,S174A,S181A,S199A,S208A (6-SA) and T360A mutants as indicated. Cells were incubated in the absence and presence of 1 nM DHT for 48 h, and luciferase activity was determined. In the lower panel, expression levels of WT and mutant pSG5-MAGE were determined by transfecting COS cells with 4 μg pSG5 empty vector (lane 1), WT pSG5-MAGE (lane 2), and the 6-SA (lane 3) and T360A (lane 4) mutants. Protein extracts (2 μg/lane) were analyzed by immunoblotting using MagAb59-79 antibody. (C) Lack of AR AF2 transcriptional response to MAGE-T360A. CV1 cells were transfected with 5 μg MMTV-Luc and 0.1 μg pCMV-ARΔ120–472 in the absence and presence of 2 μg pSG5-TIF2 and 2 μg WT pSG5-MAGE, 6-SA, and T360A mutant as indicated. Cells were incubated in the absence and presence of 1 nM DHT for 48 h, and luciferase activity was measured. (D) Lack of AR AF1 transcriptional response to MAGE-T360A. HeLa cells were transfected with 0.1 μg PSA-Enh-Luc with 0.01 μg pCMV5 empty vector (p5) and 0.01 μg pCMV-AR1-660 in the absence and presence of 0.1 μg WT pSG5-MAGE, 6-SA, or T360A mutants as indicated. Luciferase activity was measured 48 h later. (E) Phosphorylation at MAGE-11 Thr-360. COS cells were transfected with 5 μg WT pSG5-HA-MAGE-112-429 and the T360A mutant

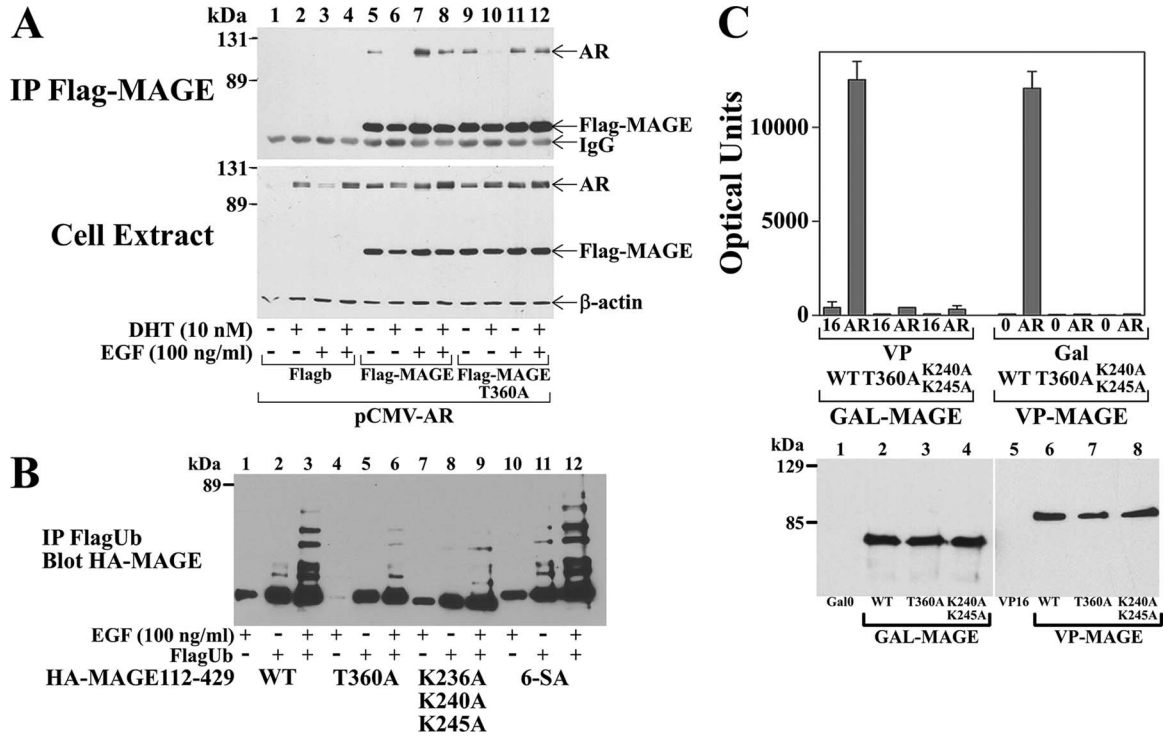

FIG. 8. Functional requirement of MAGE-11 Thr-360. (A) Reduced AR interaction with MAGE-T360A. COS cells were transfected with 2 μg pCMV-AR together with 4 μg Flagb empty vector (lanes 1 to 4), Flag-MAGE (lanes 5 to 9), or Flag-MAGE-T360A (lanes 9 to 12). The next day cells were treated for 24 h and again for 2.5 h in the absence and presence of 10 nM DHT and 100 ng/ml EGF as indicated. Transfer blots containing the immunoprecipitates (top panel) and cell extracts (15 μg protein/lane) (bottom panel) were probed with anti-Flag M2 monoclonal, AR32, and β-actin antibodies. (B) Reduced ubiquitinylation of MAGE-T360A. COS cells were transfected with 6 μg Flagb (−) and FlagUb as indicated with 3 μg wild-type (WT) pSG5-HA-MAGE-112-429 (lanes 1 to 3), and the T360A (lanes 4 to 6), K236A,K240A,K245A (lanes 7 to 9), and S168A,S170A,S174A,S181A,S199A,S208A (6-SA; lanes 10 to 12) mutants. Cells were incubated the next day in the absence and presence of 100 ng/ml EGF and 24 h later harvested for immunoprecipitation using anti-Flag affinity resin. The blot was probed using HA tag antibody. (C) Two-hybrid assay showing loss of MAGE-T360A interaction with AR. HeLa cells were transfected with 0.1 μg 5XGAL4Luc3 and 0.05 μg WT GAL-MAGE, the T360A and K240A,K245A mutants, and pVP16 empty vector or VP-AR1-660 (VP-AR) as indicated, and with 0.05 μg WT VP-MAGE and the T360A and K240A,K245A mutants with 0.05 μg GAL-0 empty vector or GAL-AR16-36 (GAL-AR) as indicated. Luciferase activity was determined 48 h later. The lower panel shows protein extracts that were analyzed by immunoblotting from COS cells transfected with 8 μg GAL-0 empty vector, WT GAL-MAGE, and the T360A and K240A,K245A mutants (50 μg protein/lane) and pVP16 empty vector, WT VP-MAGE, and the T360A and K240A,K245A mutants (60 μg protein/lane) as indicated. Transfer blots were probed using GAL-4 (left panel) and VP16 (right panel) antibodies.

We extended our studies on MAGE-11 phosphorylation to consensus threonine phosphorylation sites and found that phosphorylation at Thr-360 is essential for MAGE-11 to increase AR transcriptional activity. In contrast to wild-type MAGE-11 and the 6-SA mutant, MAGE-T360A did not increase the transcriptional activity of ARΔ120–472 assayed in the presence of TIF2 (Fig. 7C) or the constitutive activity of AR1-660 (Fig. 7D). MAGE-T360A activity was expressed at a similar level as wild-type MAGE-11 and the 6-SA mutant, and MAGE-6SA, but not MAGE-T360A, migrated slightly slower than wild-type MAGE-11 (Fig. 7B, lower panel), in agreement with the results in Fig. 7A.

In support of MAGE-11 Thr-360 phosphorylation, we found a ~2-fold increase in immunoreactivity of HA-MAGE-112-429 in response to EGF using a phosphothreonine antibody based on the ratio of phosphothreonine to HA antibody reactivity

and incubated for 24 h in the absence and presence of 100 ng/ml EGF and again in fresh medium for 2 h. Cells were extracted in IP lysis buffer, and equivalent amounts of protein were immunoprecipitated using an anti-HA affinity matrix (15 μl/470 μg protein). Immunoprecipitates were analyzed using HA tag antibody (1/10 of immunoprecipitate) and antiphosphothreonine antibody (9/10 of immunoprecipitate). Immunoblots were quantitated using an Image-Pro Plus spectrophotometer to obtain the ratio of phosphothreonine antibody to HA antibody reactivity. (F) Chk1 kinase phosphorylation of MAGE-11 Thr-360. An in vitro kinase assay was performed using GST-Chk1 kinase together with GST-^{210}GLYRSP SMPE^{219}, which is a GST-Cdc25C truncated fusion peptide substrate for Chk1 kinase (BioVision Inc.) (lane 1), GST-0 empty vector (lane 2), WT GST-MAGE-^{354}EPKRLLTQN^{362} (lane 3), and GST-MAGE-^{354}EPKRLLAQN^{362} T360A mutant (lane 4) (upper panel). Reactions were performed as described in Materials and Methods at 30°C for 30 min. The ~30-kDa band is phosphorylated WT GST-MAGE-354-362, and the ~82-kDa band appears to be autophosphorylated GST-Chk1 kinase. The rehydrated stained gel indicated equivalent protein loading (lower panel).

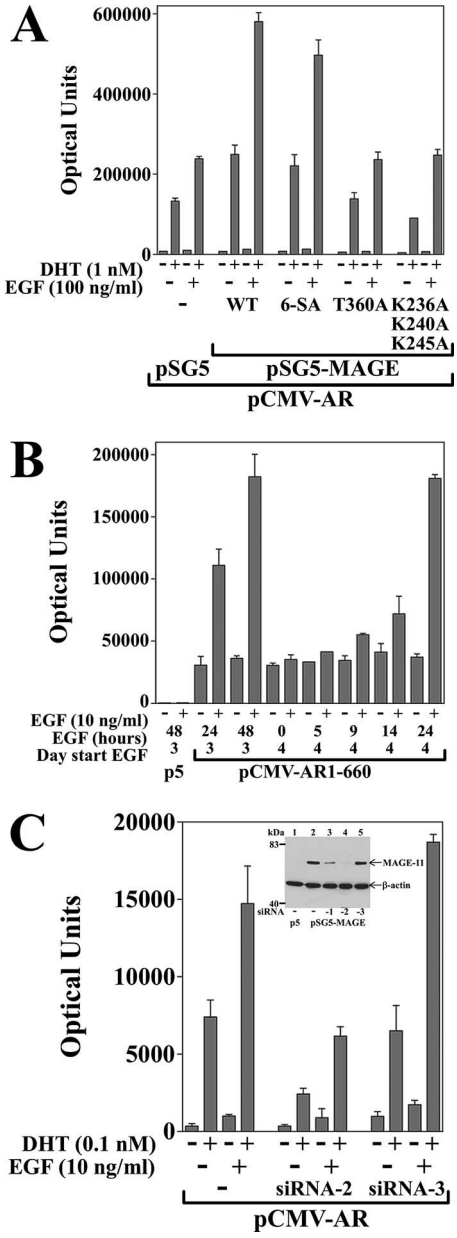

FIG. 9. Effects of MAGE-11 on AR transcriptional activity in Ishikawa cells. (A) Ishikawa cells (10^5/well in 12-well plates) were transfected using FuGENE-6 with 0.1 μg PSA-Enh-Luc, 0.01 μg pCMV-AR, and 0.1 μg pSG5, wild-type pSG5-MAGE, or the S168A,S170A, S174A,S181A,S199A,S208A (6-SA), T360A, and K236A,K240A, K245A mutants as indicated. Cells were incubated in the absence and presence of 1 nM DHT and 100 ng/ml EGF for 24 h as indicated, and luciferase activity was measured. (B) Time dependence of the EGF-induced increase in AR1-660 activity. Ishikawa cells (7.5×10^4/well) were plated (day 1) in separate 12-well plates according to the time of harvest and transfected (day 2) with 0.1 μg MMTV-Luc and 0.05 μg pCMV5 (p5) and 0.05 μg pCMV-AR1-660 as indicated using FuGENE-6. On day 3, cells were cultured in the absence and presence of 10 ng/ml EGF. The next day (day 4), the media were exchanged and cells were harvested for luciferase activity (day 3, 24 h) or further incubated for the indicated times in the absence and presence of 10 ng/ml EGF. Cells were solubilized in luciferase lysis buffer and lysates were stored at −20°C until analysis for luciferase activity, which was stable to freeze-thaw. (C) Inhibition of AR transcriptional activity by MAGE-11 siRNA. Ishikawa cells (10^5/well in 12-well plates) were transfected using Lipofectamine 2000 with 0.1 μg MMTV-Luc and 0.025 μg pCMV-AR in the absence and presence of 2 nM MAGE-11 siRNA-2 and siRNA-3 as indicated. Twenty-four h after transfection, cells were placed in serum-free, phenol red-free medium without hormone treatment. After 24 h the medium was replaced with fresh medium with and without 0.1 nM DHT and 10 ng/ml EGF as indicated. Cells were cultured another 24 h, and luciferase activity was measured. (Inset) Inhibition of MAGE-11 expression by siRNA. COS cells (4×10^5/well in six-well plates) were transfected using Lipofectamine 2000 in Dulbecco's modified Eagle's medium without antibiotics with 0.5 μg pSG5 (p5, lane 1) and 0.5 μg pSG5-MAGE in the absence (lane 2) and presence of 10 nM MAGE-11 siRNA-1 (lane 3), siRNA-2 (lane 4), and siRNA3 (lane 5). Cells were extracted in IB lysis buffer and analyzed (10 μg/lane) on immunoblots using MagAb13-26 and β-actin antibodies.

(Fig. 7E, lanes 2 and 3). Phosphothreonine antibody immunoreactivity by the HA-MAGE-112-429-T360A mutant was two- to fourfold less than wild type and was not altered by EGF (Fig. 7E, lanes 2 to 5). Based on a predicted cell cycle checkpoint Chk1 kinase phosphorylation site at MAGE-11 Thr-360, we also performed an in vitro kinase assay using a GST-Cdc25 Chk1 substrate fusion peptide as a control (Fig. 7F, lane 1) and GST-MAGE-354-362 and the corresponding T360A mutant. The MAGE-11 peptide was phosphorylated by Chk1 kinase in a site-specific manner that was eliminated by the T360A mutation (Fig. 7F, lanes 3 and 4).

In studies to test the effect of the T360A mutation on the AR-MAGE interaction, we found that coimmunoprecipitation of AR with Flag-MAGE-T360A was reduced in the presence of EGF and absence of DHT (Fig. 8A, lanes 7 and 11). However, AR remained detectable at a reduced level in the coimmunoprecipitates with Flag-MAGE-T360A in the presence of EGF alone or with EGF and DHT (Fig. 8A, upper panel), similar to that seen for MAGEΔ221–249 (Fig. 4D) and the ubiquitinylation site mutants (Fig. 6A) that lose AR coactivator function (Fig. 4C and 5A to C). The T360A mutation reduced the ubiquitinylation of MAGE-11 in the presence of EGF to an extent similar to MAGE-K236A,K240A,K245A (Fig. 8B). In two-hybrid assays, MAGE-T360A did not interact with the AR NH_2-terminal FXXLF motif-containing fragments VP-AR1-660 and GAL-AR16-36 (Fig. 8C, upper panel), even though the wild-type and mutant GAL- and VP-MAGE fusion proteins were expressed at similar levels (Fig. 8C, lower panels).

The results suggest that EGF increases AR transcriptional activity through the phosphorylation of MAGE-11 Thr-360, which targets MAGE-11 for ubiquitinylation.

Effects of MAGE-11 on AR transcriptional activity in Ishikawa cells. To further establish a link between the effects of EGF on the MAGE-11-dependent increase in AR transcriptional activity, we directed our studies to the human endometrial Ishikawa cell line. Ishikawa cells express AR and MAGE-11, but at low levels that require transient expression of AR to activate a reporter gene (2). Initially we tested the EGF dependence of AR transcriptional activity in Ishikawa cells and the functional effects of the phosphorylation and ubiquitinylation site mutants that eliminate the coactivator function of MAGE-11. We found that DHT increases AR transcriptional activity in Ishikawa cells to a greater extent in the presence of EGF (Fig. 9A). Furthermore, AR activity was enhanced by

coexpressing wild-type MAGE-11 or the 6-SA mutant in the absence and presence of EGF. However, in agreement with the results presented above, the coactivator function of MAGE-11 was abolished by the T360A and K236A,K240A,K245A mutations. The results indicate that in Ishikawa cells, the AR coactivator function of MAGE-11 requires the same MAGE-11 threonine phosphorylation and lysine ubiquitinylation sites.

To relate the time-dependent EGF-induced stabilization of the MAGE-AR-DHT complex (Fig. 1B) to the EGF-dependent increase in AR transcriptional activity in Ishikawa cells (Fig. 9A), we expressed AR1-660, the constitutively active AR NH_2-terminal and DNA binding domain fragment, without coexpressing MAGE-11. AR1-660 transcriptional activity was increased after 24 and 48 h in response to EGF, but the increase was detected only after 9 to 14 h of exposure of cells to EGF (Fig. 9B). Maximal EGF induction of AR1-660 transcriptional activity occurred between 24 and 48 h, whereas AR1-660 transcriptional activity was constant over the 48 h of culture in the absence of EGF.

The remarkably similar ~10-h time dependence of the EGF-induced increase in AR transcriptional activity (Fig. 9B) and EGF-dependent stabilization of the MAGE-AR-DHT complex (Fig. 1B) supported the possibility that EGF increased AR activity in Ishikawa cells through endogenous MAGE-11. To address this, we cotransfected Ishikawa cells with siRNA-2, which reduces MAGE-11 expression, and siRNA-3, which does not (Fig. 9C, inset). We found that siRNA-2, but not siRNA-3, reduced full-length AR transcriptional activity in the absence and presence of EGF (Fig. 9C), suggesting that the DHT- and EGF-dependent increase in AR transcriptional activity in Ishikawa cells involves endogenous MAGE-11.

DISCUSSION

Modulation of AR transcriptional activity by the N/C interaction and MAGE-11. AR transcriptional activity relies on a complex sequence of events involving a potentially large number of coregulatory proteins through mechanisms that are not well understood (29). One regulatory mechanism that modulates AR transcriptional activity is the androgen-dependent AR N/C interaction between the NH_2-terminal FXXLF motif and AF2 in the ligand binding domain (21, 26, 30, 40, 51, 57). The AR N/C interaction depends on high-affinity binding of testosterone, DHT, or synthetic anabolic steroids, which are agonists in vivo (36, 62). The functional importance of the AR N/C interaction in androgen-dependent gene regulation is supported by naturally occurring AR AF2 site mutations that cause the androgen insensitivity syndrome, reduce AR FXXLF motif binding, and increase the dissociation rate of bound androgen without altering the apparent equilibrium androgen binding affinity (15, 22, 34, 49, 57).

However, these same AF2 site mutations that disrupt AR FXXLF motif binding also inhibit AR AF2 recruitment of SRC/p160 coactivator LXXLL motifs, which bind with at least 5- to 10-fold-lower affinity than the FXXLF motifs present in AR (22, 23), putative AR coregulators (27, 32, 58), and peptides identified in peptide display screens (8, 14, 31). Crystal structures of the AR ligand binding domain bound to natural or synthetic androgen agonists have demonstrated overlapping AF2 binding sites for the FXXLF and LXXLL motifs (1, 22, 23, 32), supporting their physiological relevance in AR function. Coexpression of SRC/p160 coactivators can increase AR transcriptional activity in an LXXLL motif-dependent manner (26), even though the AR FXXLF motif binding to AF2 has an inhibitory effect on the recruitment of SRC/p160 coactivator LXXLL motifs (21). Weaker coactivator LXXLL motif binding to AR may be compensated by higher cell and tissue-specific expression levels of the SRC/p160 coactivators, as reported in prostate cancer (17). The higher-affinity AR FXXLF motif binding supports the biological importance of the AR N/C interaction and suggests a regulatory function in modulating the transcriptional effects of SRC/160 coactivators.

The apparent dual function of the AR AF2 site in establishing AR transcriptional activity is controlled in part by MAGE-11, an AR coregulator that selectively binds the FXXLF motif region of AR and competes for the AR N/C interaction. MAGE-11 increases overall AR transcriptional activity by exposing AF2 to coactivator recruitment (3) and through additional mechanisms independent of AF2. The MAGE-11-induced increase in AR transcriptional activity at enhancer elements that require the AR N/C interaction for maximal activity (3, 26) suggests a complex interrelationship between AR AF2 transcriptional activity and MAGE-11 binding that is modulated by interactions at the AR FXXLF motif.

EGF regulation of AR through MAGE-11. In this report we provide evidence that EGF cell signaling increases AR transcriptional activity through the posttranslational modification of MAGE-11. We demonstrated that EGF induces the ubiquitinylation of MAGE-11 at Lys-240 and Lys-245, two residues that are also required for MAGE-11 to interact with the AR NH_2-terminal FXXLF motif. Mutations at these residues reduce the EGF-dependent ubiquitinylation of MAGE-11 and cause MAGE-11 to lose coregulator function. In the absence of DHT and EGF, interaction of the transcriptionally inactive AR with MAGE-11 through the AR FXXLF motif depends on the ubiquitinylation of MAGE-11. AR is also detected in association with MAGE-11 at reduced levels independent of the lysine ubiquitinylation sites, raising the possibility of a second weaker interaction site not directly linked to coactivator function. Stable complex formation between AR and MAGE-11 in the absence of androgen is unimpeded by the androgen-dependent AR N/C interaction and increases AR levels, providing a mechanism for greater AR transcriptional activity in response to low levels of androgen.

In the presence of DHT, the androgen-dependent AR N/C interaction of the transcriptionally active AR competes with AR FXXLF motif binding to MAGE-11. Just as MAGE-11 stabilizes AR in the absence of androgen, AR is stabilized in the presence of androgen by the AR N/C interaction, providing a second mechanism to increase overall cell content of AR for gene activation. The transient nature of the MAGE-AR-DHT complex in the presence of DHT without EGF signaling appears to reflect this competitive relationship that is centered on the AR FXXLF motif. However, in the presence of DHT and EGF, AR transcriptional activity increases, dependent on increased ubiquitinylation of MAGE-11 and stabilization of the MAGE-AR-DHT complex.

The somewhat paradoxical effects of EGF to increase AR transcriptional activity through the stabilization of the MAGE-AR-DHT complex yet to increase MAGE-11 turnover may

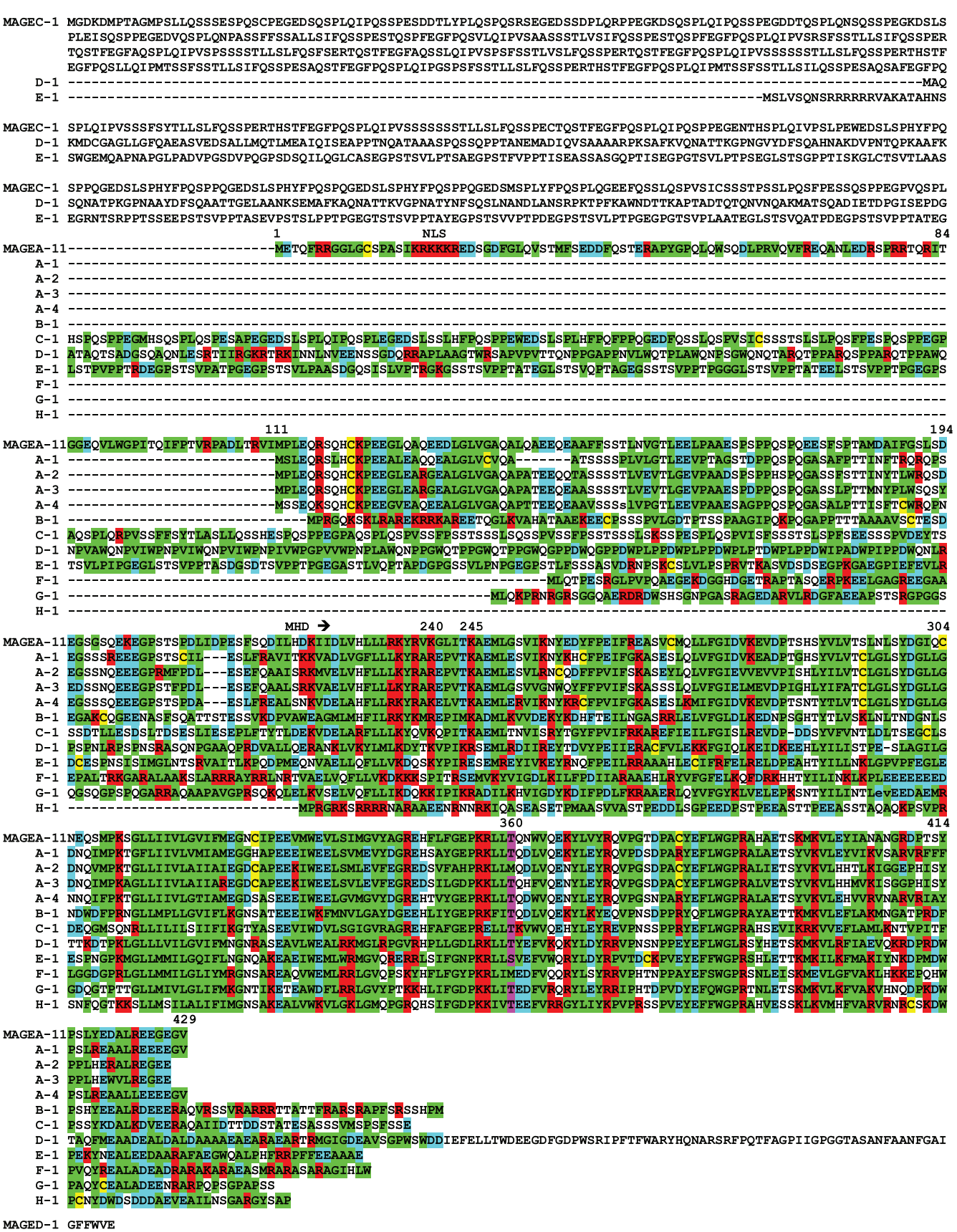

FIG. 10. Sequence alignment of the MAGE superfamily. Amino acid sequence alignment was performed using PredictProtein (http://www.predictprotein.org) and is shown for MAGE-11 of the MAGE-A subfamily, the first four members of the MAGE-A subfamily, and the primary

reflect the EGF-dependent increase in the mono- and polyubiquitinylation of MAGE-11. We provide evidence that monoubiquitinylation of MAGE-11 is required for the AR-MAGE interaction and coregulator function of MAGE-11. Increased MAGE-11 degradation in response to EGF may occur in response to polyubiquitinylation of MAGE-bound ubiquitin. The apparent inhibitory effect of the MAGE-11 NH_2-terminal region on ubiquitinylation in the absence of AR suggests that binding to AR may increase exposure of the MAGE-11 ubiquitinylation sites, leading to increased MAGE-11 turnover and greater AR transcriptional activity.

EGF-dependent stabilization of the MAGE-AR-DHT complex requires 10 h in cell culture, a time period that was also required for EGF to increase AR transcriptional activity in Ishikawa cells that express endogenous MAGE-11. It is therefore tempting to speculate that the effects of EGF on MAGE-11 are linked to progression through the cell cycle. This hypothesis gained support by evidence that MAGE-11 is phosphorylated at Thr-360 by the cell cycle checkpoint kinase Chk1. The inability of the MAGE-T360A mutant to interact with AR and increase AR transcriptional activity suggests that phosphorylation at Thr-360 by Chk1 kinase is part of a mechanism whereby EGF triggers the ubiquitinylation of MAGE-11 in association with increased AR transcriptional activity. The inability of a phosphorylation mimetic (MAGE-T360E) to rescue the interaction with AR in two-hybrid assays (data not shown) may reflect the transient nature of Thr-360 phosphorylation or the different carbon atom positions of the glutamic acid carboxyl group and threonine phosphate group. We also presented evidence for multiple serine phosphorylation sites in MAGE-11, even though none of the serine mutations diminished the ability of MAGE-11 to increase AR transcriptional or influenced the EGF-dependent ubiquitinylation of MAGE-11 and its interaction with AR. Threonine residues are estimated to be nine times less likely than serine to be sites of phosphorylation and more often serve in a signaling capacity (46).

Our results are consistent with the hypothesis that EGF increases the multiple monoubiquitinylation of MAGE-11 in association with time-dependent stabilization of the MAGE-AR-DHT complex and increased degradation of MAGE-11. EGF increases the phosphorylation and ubiquitinylation of MAGE-11, which enhances its interaction with DHT-bound AR. At the same time, EGF-dependent phosphorylation of MAGE-11 is linked to increased polyubiquitinylation and accelerated turnover of MAGE-11. While the precise sequence of events remains to be determined, EGF-dependent phosphorylation and ubiquitinylation of MAGE-11 appears to be part of a processive cycle that allows AR to release and reassociate with coactivators and the transcription complex through multiple rounds of gene activation. The effect of EGF to stabilize the DHT-bound AR interaction with MAGE-11 provides a mechanism to prolong AR-driven gene transcription.

EGF signaling and AR transcriptional activity. EGF signaling has been linked to increased AR transcriptional activity through ligand-dependent and -independent mechanisms in prostate cancer by increased coactivator recruitment (12, 13, 16, 18, 44). More recently, ubiquitin-proteasome pathways have gained attention for their role in chromatin remodeling by nuclear receptors (37) and in the phosphorylation and ubiquitinylation of RNA polymerase (4, 47). However, to our knowledge, growth factor signaling has not been linked to steroid hormone receptor regulation through the site-specific ubiquitinylation of a coregulator. Ubiquitinylation of coactivator proteins such as SRC3/AIB1 was shown to be modulated by phosphorylation and may occur in a processive manner in association with gene activation (41, 61). A similar mechanism likely occurs in AR-directed gene transcription and involves the AR N/C interaction and binding of MAGE-11.

Although we found no evidence that AR itself was ubiquitinylated in the present study, AR undergoes rapid degradation in the absence of androgen or MAGE-11 (35) and is reportedly linked to a proteosome-mediated mechanism (52) through a direct interaction between AR and the E3 ubiquitin ligase Hsp70/Hsp90 cochaperone, the carboxyl terminus of Hsp70 interacting protein (CHIP). CHIP interacts with AR through a highly conserved AR NH_2-terminal domain sequence (20). A regulatory role for CHIP in AR function is supported by the spontaneous AR somatic missense mutation AR-E231G in a mouse model of prostate cancer, which inhibits CHIP binding and may contribute to prostate neoplasia (19, 20). Whether CHIP is involved in AR modulation by MAGE-11 in normal human physiology or prostate cancer remains to be determined. AR transcriptional activity was also reported to be increased by AR monoubiquitinylation through increased interaction with coregulatory proteins (6) in association with the phosphorylation and increased degradation of AR (42).

The AR selective coregulatory function of MAGE-11 is supported by the cell and tissue expression profiles. Both AR and MAGE-11 are expressed in normal tissues of the human male and female reproductive tracts and in prostate cancer cell lines (2, 3). MAGE-11 is expressed in a temporal fashion in glandular epithelial cell nuclei of normal cycling human endometrium and is hormonally regulated during the menstrual cycle (2). MAGE-11 is down-regulated by estradiol during the proliferative phase of the human endometrium and up-regulated in response to cyclic AMP during the early and mid-secretory stage. Highest levels of MAGE-11 mRNA and protein coincide with the window of receptivity to embryo implantation, suggesting a functional link between AR and MAGE-11 in normal female fertility. Increased expression of MAGE-11 may also contribute to AR transcriptional activity in androgen-

member of MAGE subfamilies B to H. Amino acid residues are color coded for lysine and arginine (red), aspartic and glutamic acid (blue), glycine, alanine, valine, leucine, isoleucine, proline, and methionine (green), cysteine (yellow), and Thr-360 (purple). Also indicated for MAGE-11 is the nuclear localization signal (NLS, residues 18 to 23), the first and second (Met-111) methionine residues, the MAGE homology domain (MHD) residues 222 to 421, Lys-240 and Lys-245 ubiquitinylation sites, and the Thr-360 phosphorylation site. Absence of sequence and minimal interior spacing for optimal sequence alignment are designated by a dash. In two instances, lowercase letters signify deletion of an intervening proline.

dependent and castration-recurrent prostate cancer, which typically expresses AR during androgen deprivation therapy when circulating androgen levels are low.

Conservation of MAGE-11 phosphorylation and ubiquitinylation sites throughout the MAGE gene family. MAGE-11 shares extensive sequence homology with the MAGE superfamily of so-called cancer-testis antigens (Fig. 10). MAGE-11 is a member of the MAGE-A subfamily that includes 12 proteins coded at the Xq28 region of the human X chromosome (10, 50, 54). Thus, both AR and MAGE-11 are expressed on the human X chromosome (5). MAGE-11 is unique among the MAGE family by having 89 NH_2-terminal amino acid residues encoded by three short 5′ exons that include a nuclear targeting signal in the first coding exon (3, 33). All other MAGE-A family members initiate at a methionine that corresponds to Met-111 in MAGE-11 (shown for MAGE-A-1 to -4 in Fig. 10). Within the carboxyl-terminal residue 112 to 429 region of MAGE-11, which interacts with the AR FXXLF motif, is the MAGE homology domain (MAGE-11 residues 222 to 421), which is highly conserved throughout the entire MAGE gene superfamily (Fig. 10). Our results therefore support the previous suggestion that the MAGE homology domain serves as a protein-protein interaction site (56). It is also interesting that the EGF-dependent Thr-360 phosphorylation site and Lys-240 and Lys-245 ubiquitinylation sites in MAGE-11 are among the most highly conserved residues within the MAGE homology domain throughout the MAGE superfamily (Fig. 10). This raises the possibility that similar posttranslational modifications are involved in the as-yet-unknown functions of most of the MAGE gene family. The apparent lack of a functional homologue for MAGE-11 in rats and mice suggests a specialized function in human and nonhuman primate physiology to increase and prolong AR transcriptional activity through mechanisms downstream of growth factor signaling.

ACKNOWLEDGMENTS

We thank Brian J. Kennerley, John T. Minges, Andrew T. Hnat, and K. Michelle Cobb for excellent technical assistance, Frank S. French for reviewing the manuscript, David Lonard and Bert O'Malley for helpful comments and providing the lysine-free ubiquitin clone, and Stephanie L. H. Miller and John P. O'Bryan for Flag-Ub.

The work was supported by U.S. Public Health Service grants HD16910 from NICHD, U54-HD35041 cooperative agreement of the specialized Cooperative Centers Program in Reproduction and Infertility Research of the National Institutes of Health, National Institute of Child Health and Human Development, and by P01-CA77739 from the National Cancer Institute.

REFERENCES

1. **Askew, E. B., R. T. Gampe, T. B. Stanley, J. L. Faggart, and E. M. Wilson.** 2007. Modulation of androgen receptor activation function 2 by testosterone and dihydrotestosterone. J. Biol. Chem. **282:**25801–25816.
2. **Bai, S., G. Grossman, L. Yuan, B. A. Lessey, F. S. French, S. L. Young, and E. M. Wilson.** 11 December 2007, posting date. Hormone control and expression of androgen receptor coregulator MAGE-11 in human endometrium during the window of receptivity to embryo implantation. Mol. Hum. Reprod. doi:10.1093/molehr/gam080.
3. **Bai, S., B. He, and E. M. Wilson.** 2005. Melanoma antigen gene protein MAGE-11 regulates androgen receptor function by modulating the interdomain interaction. Mol. Cell. Biol. **25:**1238–1257.
4. **Beaudenon, S. L., M. R. Huacani, G. Wang, D. P. McDonnell, and J. M. Huibregtse.** 1999. Rsp5 ubiquitin-protein ligase mediates DNA damage-induced degradation of the large subunit of RNA polymerase II in *Saccharomyces cerevisiae*. Mol. Cell. Biol. **19:**6972–6979.
5. **Brown, C. J., S. J. Goss, D. B. Lubahn, D. R. Joseph, E. M. Wilson, F. S. French, and H. F. Willard.** 1989. Androgen receptor locus on the human X chromosome: regional localization to Xq11-12 and description of a DNA polymorphism. Am. J. Hum. Genet. **44:**264–269.
6. **Burgdorf, S., P. Leister, and K. H. Scheidtmann.** 2004. TSG101 interacts with apoptosis-antagonizing transcription factor and enhances androgen receptor-mediated transcription by promoting its monoubiquitination. J. Biol. Chem. **279:**17524–17534.
7. **Callewaert, L., N. Van Tilborgh, and F. Claessens.** 2006. Interplay between two hormone-independent activation domains in the androgen receptor. Cancer Res. **66:**543–553.
8. **Chang, C. Y., J. Abdo, T. Hartney, and D. P. McDonnell.** 2005. Development of peptide antagonists for the androgen receptor using combinatorial peptide phage display. Mol. Endocrinol. **19:**2478–2490.
9. **Charest, N. J., Z. X. Zhou, D. B. Lubahn, K. L. Olsen, E. M. Wilson, and F. S. French.** 1991. A frameshift mutation destabilizes androgen receptor messenger RNA in the Tfm mouse. Mol. Endocrinol. **5:**573–581.
10. **Chomez, P., O. De Backer, M. Bertrand, E. De Plaen, T. Boon, and S. Lucas.** 2001. An overview of the MAGE gene family with the identification of all human members of the family. Cancer Res. **61:**5544–5551.
11. **Choong, C. S., J. A. Kemppainen, and E. M. Wilson.** 1998. Evolution of the primate androgen receptor: a structural basis for disease. J. Mol. Evol. **47:**334–342.
12. **Craft, N., Y. Shostak, M. Carey, and C. L. Sawyers.** 1999. A mechanism for hormone-independent prostate cancer through modulation of androgen receptor signaling by the HER-2/neu tyrosine kinase. Nat. Med. **5:**280–285.
13. **Culig, Z., A. Hobisch, M. V. Cronauer, C. Radmayr, J. Trapman, A. Hittmair, G. Bartsch, and H. Klocker.** 1994. Androgen receptor activation in prostatic tumor cell lines by insulin-like growth factor-I, keratinocyte growth factor, and epidermal growth factor. Cancer Res. **54:**5474–5478.
14. **Dubbink, H. J., R. Hersmus, C. S. Verma, H. A. van der Korput, C. A. Berrevoets, J. van Tol, A. C. Ziel-van der Made, A. O. Brinkmann, A. C. Pike, and J. Trapman.** 2004. Distinct recognition modes of FXXLF and LXXLL motifs by the androgen receptor. Mol. Endocrinol. **18:**2132–2150.
15. **Ghali, S. A., B. Gottlieb, R. Lumbroso, L. K. Beitel, Y. Elhaji, J. Wu, L. Pinsky, and M. A. Trifiro.** 2003. The use of androgen receptor amino/carboxyl-terminal interaction assays to investigate androgen receptor gene mutations in subjects with varying degrees of androgen insensitivity. J. Clin. Endocrinol. Metab. **88:**2185–2193.
16. **Gregory, C. W., X. Fei, L. A. Ponguta, B. He, H. M. Bill, F. S. French, and E. M. Wilson.** 2004. Epidermal growth factor increases coactivation of the androgen receptor in recurrent prostate cancer. J. Biol. Chem. **279:**7119–7130.
17. **Gregory, C. W., B. He, R. T. Johnson, O. H. Ford, J. L. Mohler, F. S. French, and E. M. Wilson.** 2001. A mechanism for androgen receptor-mediated prostate cancer recurrence after androgen deprivation therapy. Cancer Res. **61:**4315–4319.
18. **Gregory, C. W., Y. E. Whang, W. McCall, X. Fei, Y. Liu, L. A. Ponguta, F. S. French, E. M. Wilson, and H. S. Earp.** 2005. Heregulin-induced activation of HER2 and HER3 increases androgen receptor transactivation and CWR-R1 human recurrent prostate cancer cell growth. Clin. Cancer Res. **11:**1704–1712.
19. **Han, G., G. Buchanan, M. Ittmann, J. M. Harris, X. Yu, F. J. Demayo, W. Tilley, and N. M. Greenberg.** 2005. Mutation of the androgen receptor causes oncogenic transformation of the prostate. Proc. Natl. Acad. Sci. USA **102:**1151–1156.
20. **He, B., S. Bai, A. T. Hnat, R. I. Kalman, J. T. Minges, C. Patterson, and E. M. Wilson.** 2004. An androgen receptor NH_2-terminal conserved motif interacts with carboxyl terminus of Hsp70-interacting protein CHIP. J. Biol. Chem. **279:**30643–30653.
21. **He, B., N. T. Bowen, J. T. Minges, and E. M. Wilson.** 2001. Androgen-induced NH_2- and COOH-terminal interaction inhibits p160 coactivator recruitment by activation function 2. J. Biol. Chem. **276:**42293–42301.
22. **He, B., R. T. Gampe, A. T. Hnat, J. L. Faggart, J. T. Minges, F. S. French, and E. M. Wilson.** 2006. Probing the functional link between androgen receptor coactivator and ligand binding sites in prostate cancer and androgen insensitivity. J. Biol. Chem. **281:**6648–6663.
23. **He, B., R. T. Gampe, A. J. Kole, A. T. Hnat, T. B. Stanley, G. An, E. L. Stewart, R. I. Kalman, J. T. Minges, and E. M. Wilson.** 2004. Structural basis for androgen receptor interdomain and coactivator interactions suggests a transition in nuclear receptor activation function dominance. Mol. Cell **16:**425–438.
24. **He, B., J. A. Kemppainen, J. J. Voegel, H. Gronemeyer, and E. M. Wilson.** 1999. Activation function 2 in the human androgen receptor ligand binding domain mediates interdomain communication with the NH_2-terminal domain. J. Biol. Chem. **274:**37219–37225.
25. **He, B., J. A. Kemppainen, and E. M. Wilson.** 2000. FXXLF and WXXLF sequences mediate the NH_2-terminal interaction with the ligand binding domain of the androgen receptor. J. Biol. Chem. **275:**22986–22994.
26. **He, B., L. W. Lee, J. T. Minges, and E. M. Wilson.** 2002. Dependence of selective gene activation on the androgen receptor NH_2- and COOH-terminal interaction. J. Biol. Chem. **277:**25631–25639.
27. **He, B., J. T. Minges, L. W. Lee, and E. M. Wilson.** 2002. The F*XX*LF motif

mediates androgen receptor-specific interactions with coregulators. J. Biol. Chem. **277:**10226–10235.
28. **He, B., and E. M. Wilson.** 2003. Electrostatic modulation of steroid receptor recruitment of the L*XX*LL and F*XX*LF motifs. Mol. Cell. Biol. **23:**2135–2150.
29. **Heinlein, C. A., and C. Chang.** 2002. Androgen receptor (AR) coregulators: an overview. Endocr. Rev. **23:**175–200.
30. **Hsu, C. L., Y. L. Chen, H. J. Ting, W. J. Lin, Z. Yang, Y. Zhang, L. Wang, C. T. Wu, H. C. Chang, S. Yeh, S. W. Pimplikar, and C. Chang.** 2005. Androgen receptor (AR) NH_2- and COOH-terminal interactions result in the differential influences on the AR-mediated transactivation and cell growth. Mol. Endocrinol. **19:**350–361.
31. **Hsu, C. L., Y. L. Chen, S. Yeh, H. J. Ting, Y. C. Hu, H. Lin, X. Wang, and C. Chang.** 2003. The use of phage display technique for the isolation of androgen receptor interacting peptides with (F/W)XXL(F/W) and FXXLY new signature motifs. J. Biol. Chem. **278:**23691–23698.
32. **Hur, E., S. J. Pfaff, E. S. Payne, H. Gron, B. M. Buehrer, and R. J. Fletterick.** 2004. Recognition and accommodation at the androgen receptor coactivator binding interface. PLOS Biol. **2:**e274.
33. **Irvine, R. A., and G. A. Coetzee.** 1999. Additional upstream coding sequences of MAGE-11. Immunogenetics **49:**585.
34. **Jaaskelainen, J., A. Deeb, J. W. Schwabe, N. P. Mongan, H. Martin, and I. A. Hughes.** 2006. Human androgen receptor gene ligand-binding-domain mutations leading to disrupted interaction between the N- and C-terminal domains. J. Mol. Endocrinol. **36:**361–368.
35. **Kemppainen, J. A., M. V. Lane, M. Sar, and E. M. Wilson.** 1992. Androgen receptor phosphorylation, turnover, nuclear transport, and transcriptional activation. Specificity for steroids and antihormones. J. Biol. Chem. **267:**968–974.
36. **Kemppainen, J. A., E. Langley, C. I. Wong, K. Bobseine, W. R. Kelce, and E. M. Wilson.** 1999. Distinguishing androgen receptor agonists and antagonists: distinct mechanisms of activation by medroxyprogesterone acetate and dihydrotestosterone. Mol. Endocrinol. **13:**440–454.
37. **Kinyamu, H. K., J. Chen, and T. K. Archer.** 2005. Linking the ubiquitin-proteasome pathway to chromatin remodeling/modification by nuclear receptors. J. Mol. Endocrinol. **34:**281–297.
38. **Langley, E., J. A. Kemppainen, and E. M. Wilson.** 1998. Intermolecular NH_2-/carboxyl-terminal interactions in androgen receptor dimerization revealed by mutations that cause androgen insensitivity. J. Biol. Chem. **273:**92–101.
39. **Langley, E., Z. X. Zhou, and E. M. Wilson.** 1995. Evidence for an anti-parallel orientation of the ligand-activated human androgen receptor dimer. J. Biol. Chem. **270:**29983–29990.
40. **Li, J., J. Fu, C. Toumazou, H. G. Yoon, and J. Wong.** 2006. A role of the amino-terminal (N) and carboxyl-terminal (C) interaction in binding of androgen receptor to chromatin. Mol. Endocrinol. **20:**776–785.
41. **Li, X., D. M. Lonard, S. Y. Jung, A. Malovannaya, Q. Feng, J. Qin, S. Y. Tsai, M. J. Tsai, and B. W. O'Malley.** 2006. The SRC-3/AIB1 coactivator is degraded in a ubiquitin- and ATP-independent manner by the REGγ proteasome. Cell **124:**381–392.
42. **Lin, H. K., L. Wang, Y. C. Hu, S. Altuwaijri, and C. Chang.** 2002. Phosphorylation-dependent ubiquitylation and degradation of androgen receptor by Akt require Mdm2 E3 ligase. EMBO J. **21:**4037–4048.
43. **Liu, Y., S. Majumder, W. McCall, C. I. Sartor, J. L. Mohler, C. W. Gregory, H. S. Earp, and Y. E. Whang.** 2005. Inhibition of HER-2/neu kinase impairs androgen receptor recruitment to the androgen responsive enhancer. Cancer Res. **65:**3404–3409.
44. **Lopez, G. N., C. W. Turck, F. Schaufele, M. R. Stallcup, and P. J. Kushner.** 2001. Growth factors signal to steroid receptors through mitogen-activated protein kinase regulation of p160 coactivator activity. J. Biol. Chem. **276:**22177–22182.
45. **Lubahn, D. B., D. R. Joseph, M. Sar, J. Tan, H. N. Higgs, R. E. Larson, F. S. French, and E. M. Wilson.** 1988. The human androgen receptor: complementary deoxyribonucleic acid cloning, sequence analysis and gene expression in prostate. Mol. Endocrinol. **2:**1265–1275.
46. **Mann, M., S. E. Ong, M. Grønborg, H. Steen, O. N. Jensen, and A. Pandey.** 2002. Analysis of protein phosphorylation using mass spectrometry: deciphering the phosphoproteome. Trends Biotechnol. **20:**261–268.
47. **Mitsui, A., and P. A. Sharp.** 1999. Ubiquitination of RNA polymerase II large subunit signaled by phosphorylation of carboxyl-terminal domain. Proc. Natl. Acad. Sci. USA **96:**6054–6059.
48. **Quarmby, V. E., W. G. Yarbrough, D. B. Lubahn, F. S. French, and E. M. Wilson.** 1990. Autologous down regulation of androgen receptor messenger ribonucleic acid. Mol. Endocrinol. **4:**22–28.
49. **Quigley, C. A., J. A. Tan, B. He, Z. X. Zhou, F. Mebarki, Y. Morel, M. Forest, P. Chatelain, E. M. Ritzen, F. S. French, and E. M. Wilson.** 2004. Partial androgen insensitivity with phenotypic variation caused by androgen receptor mutations that disrupt activation function 2 and the NH_2- and carboxyl-terminal interaction. Mech. Ageing Dev. **125:**683–695.
50. **Rogner, U. C., K. Wilke, E. Steck, B. Korn, and A. Poustka.** 1995. The melanoma antigen gene (MAGE) family is clustered in the chromosomal band Xq28. Genomics **29:**725–731.
51. **Schaufele, F., X. Carbonell, M. Guerbadot, S. Borngraeber, M. S. Chapman, A. A. Ma, J. N. Miner, and M. I. Diamond.** 2005. The structural basis of androgen receptor activation: intramolecular and intermolecular amino-carboxy interactions. Proc. Natl. Acad. Sci. USA **102:**9802–9807.
52. **Sheflin, L., B. Keegan, W. Zhang, and S. W. Spaulding.** 2000. Inhibiting proteasomes in human HepG2 and LNCaP cells increases endogenous androgen receptor levels. Biochem. Biophys. Res. Commun. **276:**144–150.
53. **Simental, J. A., M. Sar, M. V. Lane, F. S. French, and E. M. Wilson.** 1991. Transcriptional activation and nuclear targeting signals of the human androgen receptor. J. Biol. Chem. **266:**510–518.
54. **Simpson, A. J., O. L. Caballero, A. Jungbluth, Y. T. Chen, and L. J. Old.** 2005. Cancer/testis antigens, gametogenesis and cancer. Nat. Rev. Cancer **5:**615–625.
55. **Tan, J. A., D. R. Joseph, V. E. Quarmby, D. B. Lubahn, M. Sar, F. S. French, and E. M. Wilson.** 1988. The rat androgen receptor: primary structure, autoregulation of its messenger RNA and immunocytochemical localization of the receptor protein. Mol. Endocrinol. **2:**1276–1285.
56. **Taniura, H., M. Kobayashi, and K. Yoshikawa.** 2005. Functional domains of necdin for protein-protein interaction, nuclear matrix targeting, and cell growth suppression. J. Cell. Biochem. **94:**804–815.
57. **Thompson, J., F. Saatcioglu, O. A. Jänne, and J. J. Palvimo.** 2001. Disrupted amino- and carboxyl-terminal interactions of the androgen receptor are linked to androgen insensitivity. Mol. Endocrinol. **15:**923–935.
58. **van de Wijngaart, D. J., M. E. van Royen, R. Hersmus, A. C. Pike, A. B. Houtsmuller, G. Jenster, J. Trapman, and H. J. Dubbink.** 2006. Novel FXXFF and FXXMF motifs in androgen receptor cofactors mediate high affinity and specific interactions with the ligand-binding domain. J. Biol. Chem. **281:**19407–19416.
59. **Voegel, J. J., M. J. Heine, M. Tini, V. Vivat, P. Chambon, and H. Gronemeyer.** 1998. The coactivator TIF2 contains three nuclear receptor-binding motifs and mediates transactivation through CBP binding-dependent and -independent pathways. EMBO J. **17:**507–519.
60. **Wong, C. I., Z. X. Zhou, M. Sar, and E. M. Wilson.** 1993. Steroid requirement for androgen receptor dimerization and DNA binding: modulation by intramolecular interactions between the NH_2-terminal and steroid binding domains. J. Biol. Chem. **268:**19004–19012.
61. **Wu, R. C., Q. Feng, D. M. Lonard, and B. W. O'Malley.** 2007. SRC-3 coactivator functional lifetime is regulated by a phospho-dependent ubiquitin time clock. Cell **129:**1125–1140.
62. **Zhou, Z. X., M. V. Lane, J. A. Kemppainen, F. S. French, and E. M. Wilson.** 1995. Specificity of ligand-dependent androgen receptor stabilization: receptor domain interactions influence ligand dissociation and receptor stability. Mol. Endocrinol. **9:**208–218.